SDAC-TR-78-6

SHORT PERIOD S WAVE ATTENUATION UNDER THE UNITED STATES

Z.A. Der, E. Smart, and A.H. Chaplin

Seismic Data Analysis Center

Teledyne Geotech, 314 Montgomery Street, Alexandria Virginia 22314

29 September 1978

APPROVED FOR PUBLIC RELEASE; DISTRIBUTION UNLIMITED.

Sponsored by

The Defense Advanced Research Projects Agency (DARPA)

DARPA Order No. 2551

Monitored By

AFTAC/VSC

312 Montgomery Street, Alexandria, Virginia 22314

Disclaimer: Neither the Defense Advanced Research Projects Agency nor the Air Force Technical Applications Center will be responsible for information contained herein which has been supplied by other organizations or contractors, and this document is subject to later revision as may be necessary. The views and conclusions presented are those of the authors and should not be interpreted as necessarily representing the official policies, either expressed or implied, of the Defense Advanced Research Projects Agency, the Air Force Technical Applications Center, or the US Government.

Unclassified

SECURITY CLASSIFICATION OF THIS PAGE (When Data Entered)

REPORT DOCUMENTATION PAGE

READ INSTRUCTIONS BEFORE COMPLETING FORM

(14) 1. REPORT NUMBER: SDAC-TR-78-6

2. GOVT ACCESSION NO.: AD-A096449

3. RECIPIENT'S CATALOG NUMBER:

(6) 4. TITLE (and Subtitle): SHORT PERIOD S WAVE ATTENUATION UNDER THE UNITED STATES

(9) 5. TYPE OF REPORT & PERIOD COVERED: Technical rept.,

6. PERFORMING ORG. REPORT NUMBER:

(10) 7. AUTHOR(s): Eugene Smart, Zoltan Der, Audrey Chaplin

(15) 8. CONTRACT OR GRANT NUMBER(s): F08606-78-C-0007, ARPA Order-2551

9. PERFORMING ORGANIZATION NAME AND ADDRESS:
Teledyne Geotech
314 Montgomery Street
Alexandria, Virginia 22314

10. PROGRAM ELEMENT, PROJECT, TASK AREA & WORK UNIT NUMBERS:
VT/8709 (12) 74

(11) 11. CONTROLLING OFFICE NAME AND ADDRESS:
Defense Advanced Research Projects Agency
Nuclear Monitoring Research Office
1400 Wilson Blvd., Arlington, Virginia 22209

12. REPORT DATE: 29 Sep[illegible] 1978

13. NUMBER OF PAGES: 72

14. MONITORING AGENCY NAME & ADDRESS (if different from Controlling Office):
VELA Seismological Center
312 Montgomery Street
Alexandria, Virginia 22314

15. SECURITY CLASS. (of this report):

15a. DECLASSIFICATION/DOWNGRADING SCHEDULE:

16. DISTRIBUTION STATEMENT (of this Report)

APPROVED FOR PUBLIC RELEASE; DISTRIBUTION UNLIMITED.

17. DISTRIBUTION STATEMENT (of the abstract entered in Block 20, if different from Report)

18. SUPPLEMENTARY NOTES

Author's Report Date 03/07/78

19. KEY WORDS (Continue on reverse side if necessary and identify by block number)

Anelastic Attenuation
Body Wave Magnitude
United
Short Period S

20. ABSTRACT (Continue on reverse side if necessary and identify by block number)

Investigation of short period S wave spectra revealed severe attenuation of high frequency energy under the Western United States (WUS). The average Q for short period S is about three times that of P, indicating that most - if not all - anelastic losses occur in shear deformation. The Q for the Nevada Test Site appeared to be similar to the rest of the WUS.

DD FORM 1 JAN 73 1473 EDITION OF 1 NOV 65 IS OBSOLETE

Unclassified

SECURITY CLASSIFICATION OF THIS PAGE (When Data Entered)

JOB

4/08258

SHORT PERIOD S WAVE ATTENUATION UNDER THE UNITED STATES

SEISMIC DATA ANALYSIS CENTER REPORT NO.: SDAC-TR-78-6

AFTAC Project Authorization No.:	VELA T/8709
Project Title:	Seismic Data Analysis Center
ARPA Order No.:	2551
Name of Contractor:	TELEDYNE GEOTECH
Contract No.:	F08606-78-C-0007
Date of Contract:	01 October 1977
Amount of Contract:	$2,674,245
Contract Expiration Date:	30 September 1978
Project Manager:	Robert R. Blandford (703) 836-3882

P. O. Box 334, Alexandria, Virginia 22313

APPROVED FOR PUBLIC RELEASE; DISTRIBUTION UNLIMITED.

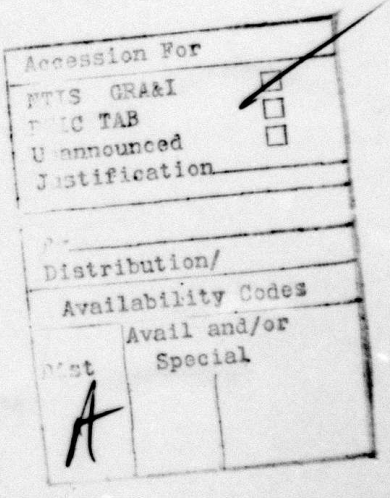

ABSTRACT

Investigation of short period S wave spectra revealed severe attenuation of high frequency energy under the Western United States (WUS). The average t^*_s (for short period S) is about three times that of P, indicating that most - if not all - anelastic losses occur in shear deformation. The t^*_s for the Nevada Test Site appeared to be similar to the rest of the WUS.

TABLE OF CONTENTS

	Page
ABSTRACT	3
LIST OF FIGURES	5
LIST OF TABLES	8
INTRODUCTION	9
Attenuation Studies of Long Period Seismic Waves	11
Study of Regional Distribution of S Wave Attenuation in the Mantle Under North America	12
DATA	14
Regional Study	14
Observed Regional t_s^* Variations and Focal Mechanisms	40
Data From the NTS Experiment	44
CONCLUSIONS	66
ACKNOWLEDGEMENT	70
REFERENCES	71

LIST OF FIGURES

Figure No.	Title	Page
1	Vertical component waveforms of short period S from the Argentine event at various LRSM stations.	21
2	Radial component waveforms of short period S from the Argentine event at various LRSM stations.	22
3	Transverse component waveforms of short period S from the Argentine event at various LRSM stations.	23
4	Vertical component waveforms of short period S from the W. Brazil event at various LRSM stations.	24
5	Radial component waveforms of short period S from the W. Brazil event at various LRSM stations.	25
6	Transverse component waveforms of short period S from the W. Brazil event at various LRSM stations.	26
7	Vertical component waveforms of short period S from the Kurile Islands event at various LRSM stations.	27
8	Radial component waveforms of short period S from the Kurile Islands event at various LRSM stations.	28
9	Transverse component waveforms of short period S from the Kurile Islands event at various LRSM stations.	29
10	Power spectra of the radial component of short period S at various LRSM stations, Argentine event. (WUS)	32
11	Power spectra of the radial component of short period S at various LRSM stations, Argentine event. (EUS)	33
12	Power spectra of the transverse component of short period S at various LRSM stations, Argentine event. (WUS)	34
13	Power spectra of the transverse component of short period S at various LRSM stations, Argentine event. (EUS)	35
14	Power spectra of the radial component of short period S at various LRSM stations, W. Brazil event.	36
15	Power spectra of the transverse component of short period S at various LRSM stations, W. Brazil event.	37
16	Power spectra of the radial component of short period S at various LRSM stations, Kurile Islands event.	38

LIST OF FIGURES (Continued)

Figure No.	Title	Page
17	Power spectra of the transverse component of short period S at various LRSM stations, Kurile Islands event.	39
18	Composite focal mechanism of Argentine events with US stations superposed (after Mendiguren). Station designation is given in Table VIII.	41
19	Focal mechanism of the Kurile event (after Veith) with US stations superposed. Station designation is given in Table VIII.	42
20	Focal mechanism of a 9 Nov 1963 W. Brazil event with US stations superposed. Station designation is given in Table VIII.	45
21	Focal mechanism of a 10 Nov 1963 W. Brazil event with US stations superposed. Station designation is given in Table VIII.	46
22	Short and long period focal mechanisms of the 9 Nov 1963 W. Brazil event (after Berckhemer and Jacob, 1968).	47
23	Short and long period focal mechanisms of the 10 Nov 1963 W. Brazil event (after Berckhemer and Jacob, 1968).	48
24	Time traces, power spectra and power spectral ratios for short period S waves observed at SDCS stations RKON and OB2NV, 19 June 1977 event, transverse component.	50
25	Time traces, power spectra and power spectral ratios for short period S waves observed at SDCS stations RKON and OB2NV, 21 April 1977 event, transverse component.	51
26	Time traces, power spectra and power spectral ratios for short period S waves observed at SDCS stations RKON and OB2NV, 4 September 1977 event, transverse component.	52
27	Time traces, power spectra and power spectral ratios for short period S waves observed at SDCS stations RKON and OB2NV, 4 September 1977 event, transverse component.	53
28	Time traces, power spectra and power spectral ratios for short period S waves observed at SDCS stations RKON and OB2NV, 21 April 1977 event, radial component.	54
29	Time traces, power spectra and power spectral ratios for short period S waves observed at SDCS stations RKON and OB2NV, 19 June 1977 event, radial component.	55

LIST OF FIGURES (Continued)

Figure No.	Title	Page
30	Time traces, power spectra and power spectral ratios for short period S waves observed at SDCS stations RKON and OB2NV, 4 September 1977 event, radial component.	[illegible]
31	Time traces, power spectra and power spectral ratios for short period S waves observed at SDCS stations RKON and OB2NV, 4 September 1977 event, radial component.	[illegible]
32	Time traces, power spectra and power spectral ratios for short period S waves observed at SDCS stations FANV and OB2NV, 19 June 1977 event, transverse component.	[illegible]
33	Time traces, power spectra and power spectral ratios for short period S waves observed at SDCS stations FANV and OB2NV, 24 July 1977 event, transverse component.	59
34	Time traces, power spectra and power spectral ratios for short period S waves observed at SDCS stations FANV and OB2NV, 19 June 1977 event, radial component.	60
35	Time traces, power spectra and power spectral ratios for short period S waves observed at SDCS stations FANV and OB2NV, 17 June 1977 event, radial component.	61
36	Time traces, power spectra and power spectral ratios for short period S waves observed at SDCS stations GBNM and OB2NV, 19 June 1977 event, transverse component.	62
37	Time traces, power spectra and power spectral ratios for short period S waves observed at SDCS stations GBNM and OB2NV, 19 June 1977 event, radial component.	63

LIST OF TABLES

Table No.	Title	Page
I	List of events used in the regional t_s^* study.	13
II	Spectral slopes in magnitude units/cps of short-period S-waves, transverse components, from the Argentine event as recorded at several LRSM sites in WUS and EUS.	15
III	Spectral slopes in magnitude units/cps of short-period S-waves, transverse components, from the western Brazil event as recorded at several sites in WUS and EUS.	16
IV	Spectral slopes in magnitude units/cps of short-period S-waves, transverse components, from the event near Kuriles as recorded at several sites in WUS and EUS.	17
V	Spectral slopes in magnitude units/cps of short-period S-waves, radial components, from the event in Argentina as recorded at several LRSM sites in WUS and EUS.	18
VI	Spectra slopes in magnitude units/cps of short-period S-waves, radial components, from the event in western Brazil as recorded at several sites in WUS and EUS.	19
VII	Spectral slopes in magnitude units/cps of short-period S-waves, radial components, from the event near Kuriles as recorded at several sites in WUS and EUS.	20
VIII	Explanation of station symbols in the focal mechanism plots.	43
IX	Epicentral data of events used at SDCS stations.	49
X	Relative Δt^* for short-period S-waves as seen at RKON and OB2NV.	64
XI	Relative Δt^* for short-period S-waves as seen at FANV and OB2NV.	65
XII	Relative Δt^* for short-period S-waves as seen at GBNM and OB2NV.	66

INTRODUCTION

Previous studies have confirmed the existence of high anelastic attenuation of seismic waves in the upper mantle under the Western part of North America. The attenuation of long period waves was studied by Solomon and Toksöz (1970), who found a region of high attenuation for P and S waves that coincided with the mountainous regions of western North America between low attenuation regions of eastern North America and a strip of low attenuation along the Pacific coast. Their study also indicated another, though less certain, high attenuation region in the northeastern United States. Studies of magnitudes from short-period P waves (Guyton, 1964; Evernden and Clark, 1970; North, 1976) revealed a low magnitude anomaly for teleseismic arrivals in western United States (WUS). Studies of spectra of short-period P waves showed that the relative high frequency content of P waves is reduced in the WUS. The observed magnitude anomaly can be explained by the simple attenuation law of

$$\exp(-\pi f t_p^*),$$

(Der and McElfresh, 1977; Der, 1976), where f is the frequency and $t_p^* = T_p/Q_p$, the ratios of P wave travel time T_p to the average quality factor Q_p for the

---

Solomon, S. C. and M. N. Toksöz (1970). Lateral variations of attenuation of P and S waves beneath the United States, Bull. Seism. Soc. Am., 60, 819-838.

Guyton, J. W. (1964). Systematic deviations of magnitude from body waves at seismograph stations in the United States, Proc. VESIAC Conf. Seismic Event Magnitude Determination, University of Michigan, 4410-71-N.

Evernden, J. and D. M. Clark (1970). Study of teleseismic P. II amplitude data, Phys. Earth Planet. Interiors, 4, 24-31.

North, R. G. (1977). Station magnitude biases-its determination, causes, and effects, Lincoln Laboratory, M.I.T. Technical Note 1977-24, 62.

Der, Z. A. and T. W. McElfresh (1977). The relationship between anelastic attenuation and regional amplitude anomalies of short-period P waves in North America, Bull. Seism. Soc. Am., 67, 1303-1317.

Der, Z. A. (1976). On the existence, magnitude and causes of broad regional variations in body-wave amplitudes (magnitude bias), SDAC-TR-76-8, Teledyne Geotech, Alexandria, Virginia 22314.

ray path. The differential in t^*_p between the eastern and western half of the continent was found to be about 0.2. Moreover, this degree of attenuation for short-period waves differed from the attenuation Solomon and Toksöz (1970) found. Because the t* differential for long period waves was several times greater than in the short-period band, the low attenuation region along the Pacific coast must either be absent or much smaller in area for short period waves. This hypothesis, if confirmed, indicates frequency dependence of t*.

Solomon and Toksöz (1970) found that t* for long period S waves was about four times that for P waves. This indicated that the anelastic losses occur mostly in shear deformation and that losses in compression are negligible. Although the regional pattern in anelastic attenuation characteristics of the upper mantle is fairly well established for short-period P waves, measuring attenuation at a single station is much more uncertain. Local geology can amplify the P wave amplitudes and, to a lesser degree, modify the spectra. This amplification was found to be quite great in the recently conducted NTS experiment (Der et al, 1977) at sites with sedimentary or tuff cover. Evaluating attenuation under NTS is especially important because most empirical knowledge of m_b-yield was accumulated at NTS and its usefulness in evaluating events worldwide cannot be assumed a priori.

This report presents results of a study of S wave attenuation across North America. Although S waves themselves are of little interest in m_b-yield work they may help, in conjunction with P wave spectral studies, to solve the following problems:

1) The separation of attenuation effects from modifications (by near surface geology) of spectra and amplitudes by providing an independent set of data: the 4:1 relation to be expected for S and P waves t* values (t^*_s and t^*_p. Solomon and Toksöz, 1970). This can help to define the magnitude of t^*_p precisely, if one assumes losses in shear only.
2) The ratio t^*_s/t^*_p is diagnostic of attenuation mechanism if losses also occur in compression.
3) The size of t^*_s in the short versus long period bands may decide the question of frequency dependence of Q_α and Q_s.
4) Resolution of the apparent discrepancy between geographical

distribution and attenuation in the long period and short period bands.

Attenuation Studies of Long Period Seismic Waves

Attenuation of seismic waves within the long and ultra long period band was studied extensively in the past. The studies fall into three basic categories: studies of selected body wave phases over specific paths; studies of surface wave trains; and free oscillations of the earth. These are, of course, three ways to look at the same thing. Early studies stressed the radial distribution of Q without any attempt to assess regional variations, and the values of t* in the various studies vary widely. Some of the variations may have been due to regional variations of Q, but most of it must have come from considerable uncertainties of spectral measurements or biases inherent in the methods of data analysis. t* is a convenient parameter to work with since it changes little with epicentral distance beyond $\Delta^\circ \sim 30^\circ$. This constancy of t* is due to the fact that most of the attenuation occurs in the upper mantle. Solomon (1972) has suggested that attenuation of long-period waves may be distributed over a greater depth range below the upper-mantle low velocity zone. Although a depth distribution such as Solomon suggested may exist at shallower depths, studies of long-period wave amplitudes showed that the decrease of teleseismic wave amplitudes is determined solely by the geometrical ray divergence, indicating negligible anelastic attenuation in the deeper mantle (Sengupta and Toksöz, 1977).

Study of Regional Distribution of S Wave Attenuation in the Mantle Under North America

To initiate this study we set out to measure the average regional differential in t_s^* in the short-period band between the eastern and western halves of North America, separated by a line along the Rocky Mountain front

---

Solomon, S. C. (1972). Seismic-wave attenuation and partial melting in the upper mantle of North America, J. Geophys. Res., 77, 1483-1502.

Sengupta, M. K. and M. N. Toksöz (1977). The amplitudes of P waves and magnitude corrections for deep focus earthquakes, J. Geophys. Res., 82, 2071-20.

ranges. (Der et al., 1975); some of the S wave data from this study has been digitized. The events and stations used are given in Table I. The three short-period components of the seismograms of these events were digitized from analog tape at 20 samples/second. The data were rotated into SV and SH components and the two components of S were analyzed separately.

Der, Z. A., R. P. Massé and J. P. Gurski (1975). Regional attenuation of short-period P and S waves in the United States, Geophys. J., 40, 85-106.

TABLE I

List of events used in the regional t_s^* study.

Date	Region	Latitude	Longitude	Magnitude	Depth (km)	Origin Time
1962 Sept. 29	Argentina	27.0S	63.6W	6.5	575	15:17:47.7
1964 March 18	NW Kuriles	52.5N	153.6E	5.6	400	04:37:26.9
1964 Nov. 28	Western Brazil	7.7S	71.2W	5.4	626	16:41:33.4

DATA

Regional Study

Three deep-focus events previously studied by Der et al. (1975) have been selected for spectral analyses. The remaining events in that paper possessed too low an S/N ratio and, therefore, were not suitable for spectral analysis. The events are listed in Table I. The seismograms containing S wave arrivals were digitized from analog tapes at 20 samples/second and rotated into vertical, radial and transverse components. A time window 25.6 seconds long was taken to analyze a given signal starting 4 seconds before the arrival of the S wavetrain. The waveform within the window was tapered using Parzen's windowing function and then was Fourier transformed. The resulting spectra were smoothed with a moving 12 point average. A noise window prior to the signal was similarly treated.

Straight lines were fitted to the logarithms of amplitude spectra, disregarding the points where the signal to noise power ratio was less than 3. The slopes of log-amplitude versus frequency are listed in Tables II to VII. The slopes of line fits to the logarithms of spectra are, by themselves, meaningless. The slopes will depend upon many factors such as source spectra, focal mechanism, instrument responses, and attenuation. Between two stations measuring the same event, the difference in slopes is proportional to the difference in t_s^*.

Figures 1 through 9 show the waveforms of all components of S mounted around the map of the United States with pointers indicating the position of the recording station. These figures demonstrate the tendency of the WUS stations to have larger dominant S wave periods than those of the EUS stations. Much of the high frequency energy evident in the EUS is not present in the WUS. The vertical is the smallest component of motion. Plot normalization is such that three plotted components of motion are comparable at a single station, but not between stations.

In dominant wave periods the visual difference is greatest for the Argentine event because of the fairly flat source spectrum within the frequency band of the short period instrument. The highest S wave frequencies are present

TABLE II

Spectral slopes in magnitude units/cps of short-period S-waves, transverse components, from the Argentine event as recorded at several LRSM sites in WUS and EUS.

WUS Spectral Slope		EUS Spectral Slope	
CPCL	-2.19	AYSD	-0.62
DRCO	-2.81	BLWV	-0.95
HLID	-1.61	CTOK	-0.56
KNUT	-3.50	CVNT	-0.69
MNNV	-1.16	DHNY	-0.50
MVCL	-1.84	GVTX	-0.99
TFCL	-1.79	HBOK	-1.09
		HTMN	-0.98
		MPAR	-0.63
		SEMN	-0.52
		SJTX	-0.86
		SSTX	-1.03
		TUPA	-0.81

mean	$\mu_w = -2.129$	$\mu_e = -0.787$
std. dev.	$s = 0.791$	$s = 0.210$
std. dev. of mean	$s_m = 0.299$	$s_m = 0.058$

difference of means $\mu_w - \mu_e = -1.342 \pm 0.609$

std. dev. of difference in means $s = 0.305$

$\Delta t_s^* = +0.984 \pm 0.446$ 95% confidence interval

TABLE III

Spectral slopes in magnitude units/cps of short-period S-waves, transverse components, from the western Brazil event as recorded at several sites in WUS and EUS.

WUS Spectral Slope		EUS Spectral Slope	
GEAZ	-1.71	BLWV	-0.58
KNUT	-2.21	FOTX	-0.17
LCNM	-0.93	GVTX	-1.03
RTNM	-2.41	RKON	-0.52
		RYND	-1.01
		VOIO	-0.57

mean	$\mu_w = -1.815$	$\mu_e = -0.646$
std. dev.	$s = 0.658$	$s = 0.324$
std. dev. of mean	$s_m = 0.329$	$s_m = 0.132$

difference of means $\mu_w - \mu_e = -1.169 \pm 0.709$

std. dev. of difference in means $s = 0.355$

$\Delta t_s^* = +0.857 \pm 0.520$ 95% confidence interval

TABLE IV

Spectral slopes in magnitude units/cps of short-period S-waves, transverse components, from the event near Kuriles as recorded at several sites in WUS and EUS.

WUS	Spectral Slope	EUS	Spectral Slope
DRCO	-2.17	BLWV	-0.82
EKNV	-1.46	DHNY	-0.76
FRMA	-2.25	HNME	-1.01
GIMA	-1.86	RYND	-1.67
KMCL	-1.87		
KNUT	-2.10		
LCNM	-3.10		
MNNV	-2.00		

mean	$\mu_w = -2.101$	$\mu_e = -1.065$
std. dev.	$s = 0.473$	$s = 0.420$
std. dev. of mean	$s_m = 0.167$	$s_m = 0.210$

difference of means $\mu_w - \mu_e = -1.036 \pm 0.537$

std. dev. of difference of means $s = 0.269$

$\Delta t_s^* = +0.759 \pm 0.394$ 95% confidence interval

TABLE V

Spectral slopes in magnitude units/cps of short-period S-waves, radial components, from the event in Argentina as recorded at several LRSM sites in WUS and EUS.

WUS	Spectral Slope	EUS	Spectral Slope
CPCL	-1.490	AYSD	-0.720
DRCO	-2.090	BLWV	-0.535
HLID	-1.885	CTOK	-0.625
KNUT	-2.800	CVNT	-0.595
MNNV	-1.170	DHNY	-1.025
MVCL	-1.160	GVTX	-0.685
TFCL	-1.225	HBOK	-1.405
		HTMN	-0.530
		MPAR	-0.305
		SEMN	-0.840
		SJTX	-0.940
		SSTX	-1.220
		TUPA	-1.035

mean	$\mu_w = -2.129$	$\mu_e = -0.787$
std. dev.	$s = 0.791$	$s = 0.210$
std. dev. of mean	$s_m = 0.299$	$s_m = 0.058$

difference of means $\mu_w - \mu_e = -1.342 \pm 0.609$

std. dev. of difference in means $s = 0.305$

$\Delta t_s^* = +0.984 \pm 0.446$ 95% confidence interval

TABLE VI

Spectral slopes in magnitude units/cps of short-period S-waves, radial components, from the event in western Brazil as recorded at several sites in WUS and EUS.

WUS	Spectral Slope	EUS	Spectral Slope
GEAZ	-1.04	BLWV	-1.14
KNUT	-2.24	FOTX	-1.32
LCNM	-0.76	GVTX	-1.02
RTNM	-0.90	RKON	-0.56
		RYND	-0.53
		VOIO	-0.64

mean	$\mu_w = -1.235$	$\mu_e = -0.868$
std. dev.	$s = 0.680$	$s = 0.335$
std. dev. of mean	$s_m = 0.340$	$s_m = 0.137$

difference of means $\mu_w - \mu_e = -0.367 \pm 0.733$

std. dev. of difference in means $s = 0.367$

$\Delta t_s^* = +0.269 \pm 0.537$ 95% confidence interval

TABLE VII

Spectral slopes in magnitude units/cps of short-period S-waves, radial components, from the event near Kuriles as recorded at several sites in WUS and EUS.

WUS	Spectral Slope	EUS	Spectral Slope
DRCO	-1.820	BLWV	-0.680
EKNV	-1.255	DHNT	-0.615
FRMA	-0.715	HNME	-0.615
GIMA	-1.145	RYND	-1.670
KMCL	-0.865		
KNUT	-2.935		
LCNM	-2.495		
MNNV	-1.425		

mean	$\mu_w = -1.582$	$\mu_e = -0.895$
std. dev.	$s = 0.785$	$s = 0.518$
std. dev. of mean	$s_m = 0.277$	$s_m = 0.259$

difference of means $\mu_w - \mu_e = -0.687 \pm 0.758$

std. dev. of difference of means $s = 0.379$

$\Delta t^*_s = +0.504 \pm 0.556$ 95% confidence interval

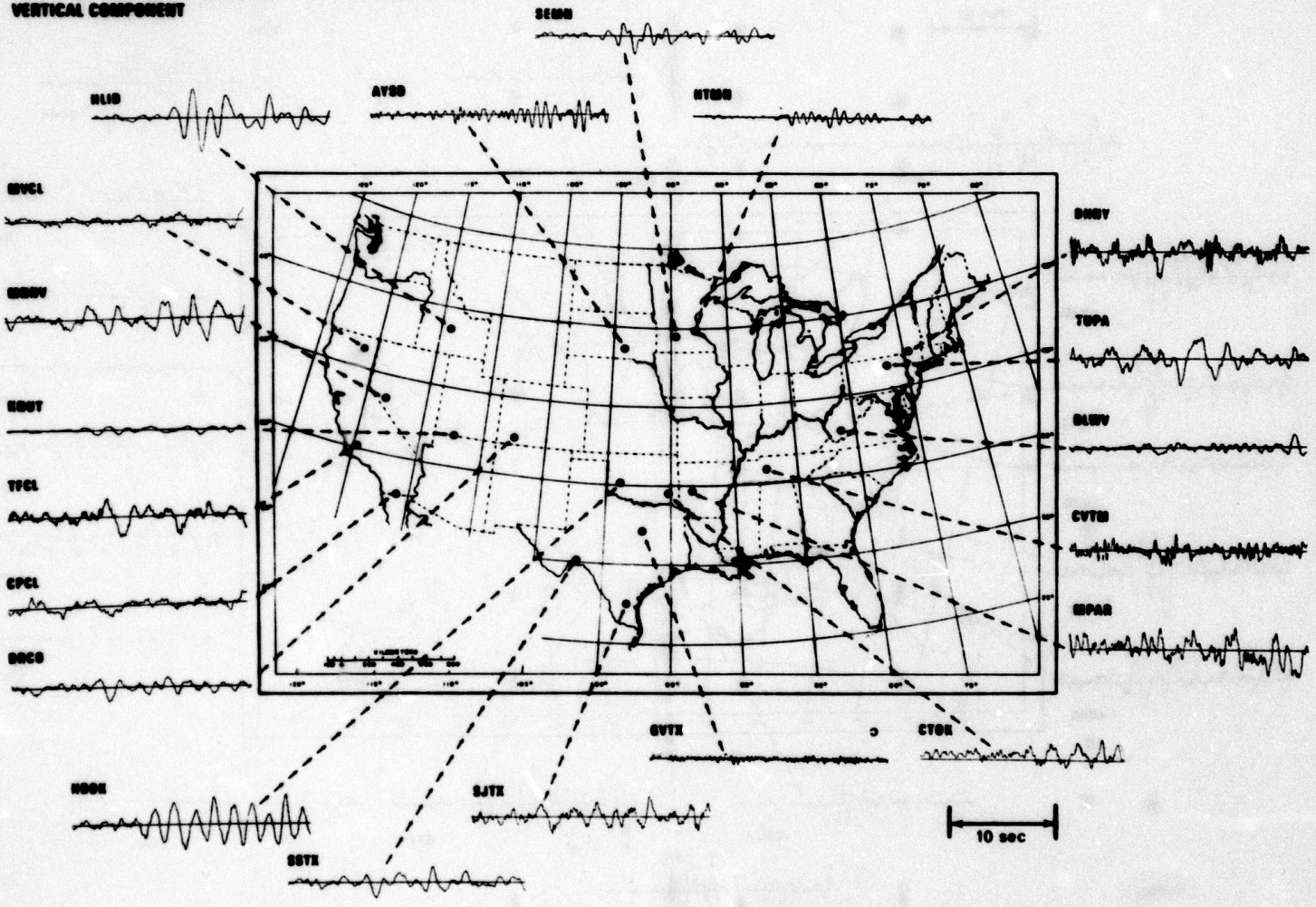

Figure 1. Vertical component waveforms of short period S from the Argentine event at various LRSM stations.

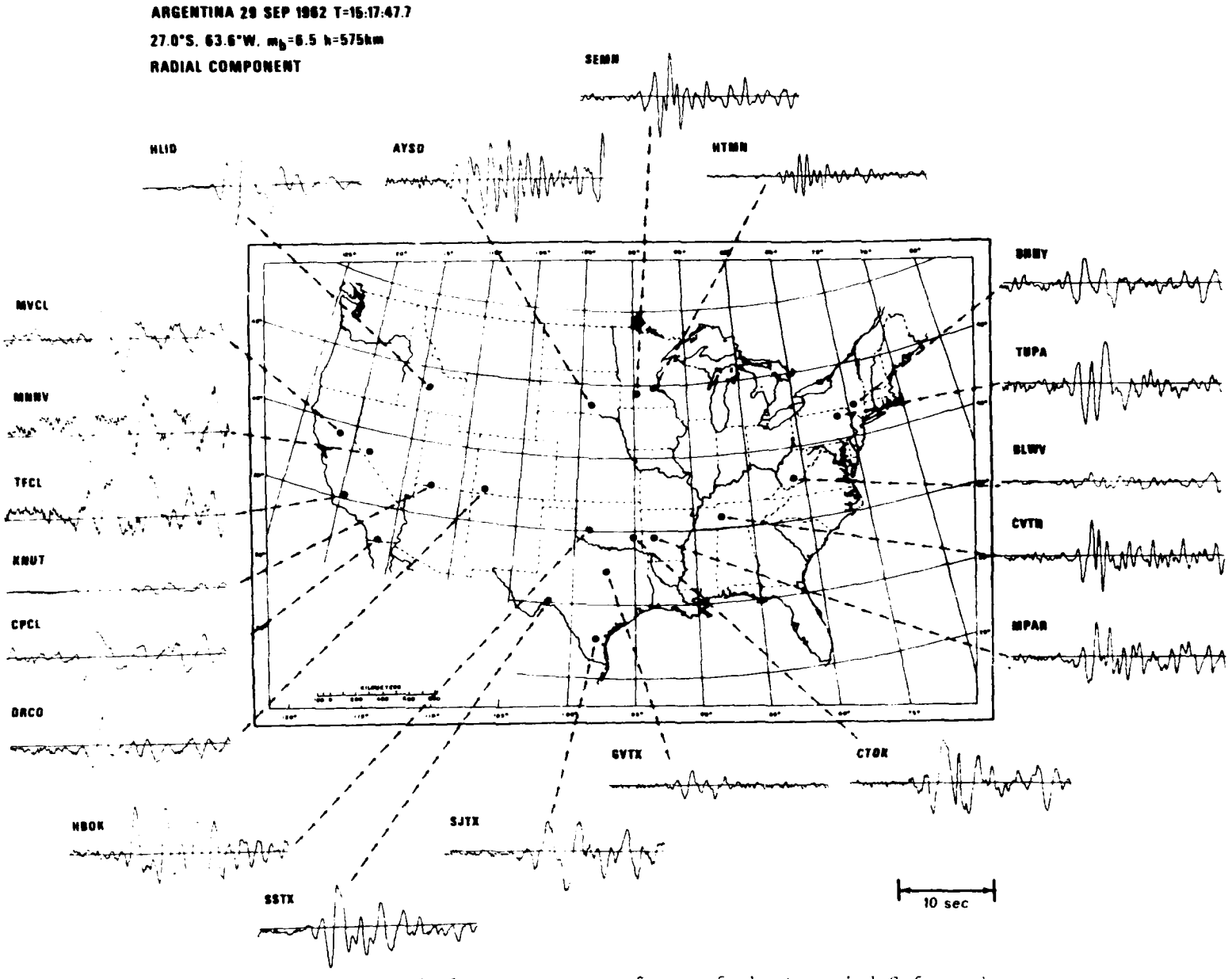

Figure 2. Radial component waveforms of short period S from the Argentine event at various LRSM stations.

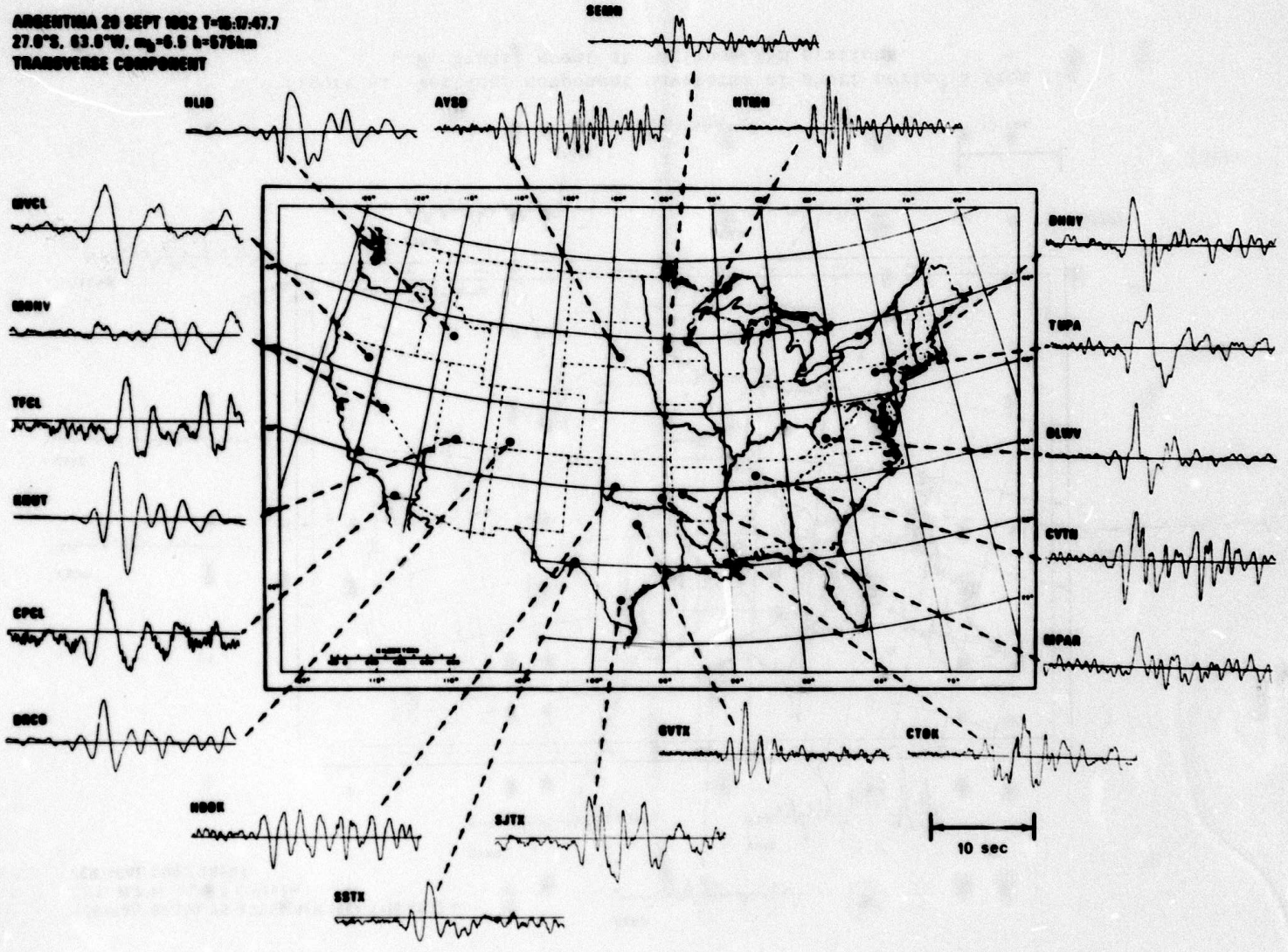

Figure 3. Transverse component waveforms of short period S from the Argentine event at various LRSM stations.

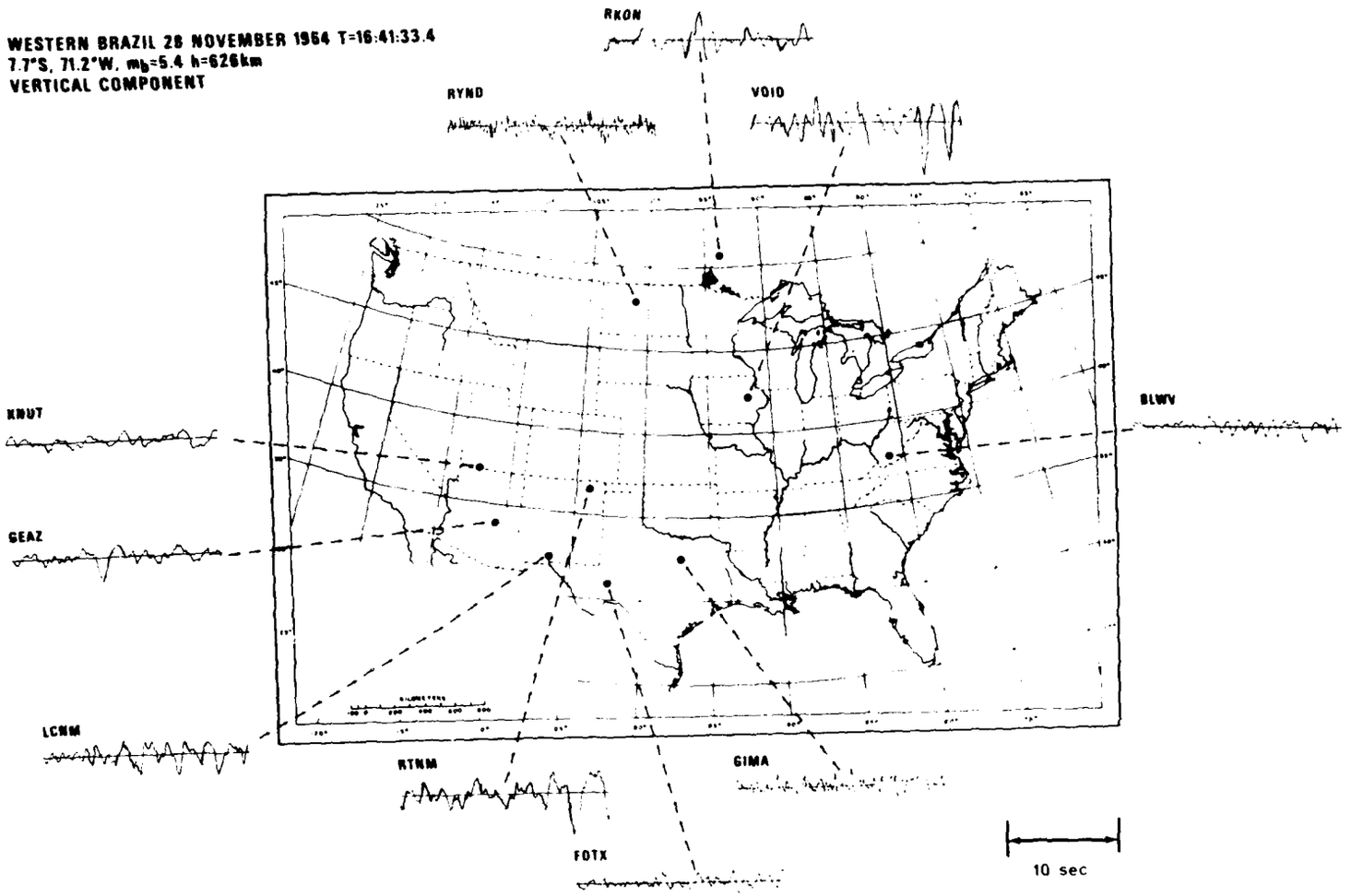

Figure 4. Vertical component waveforms of short period S from the W. Brazil event at various LRSM stations.

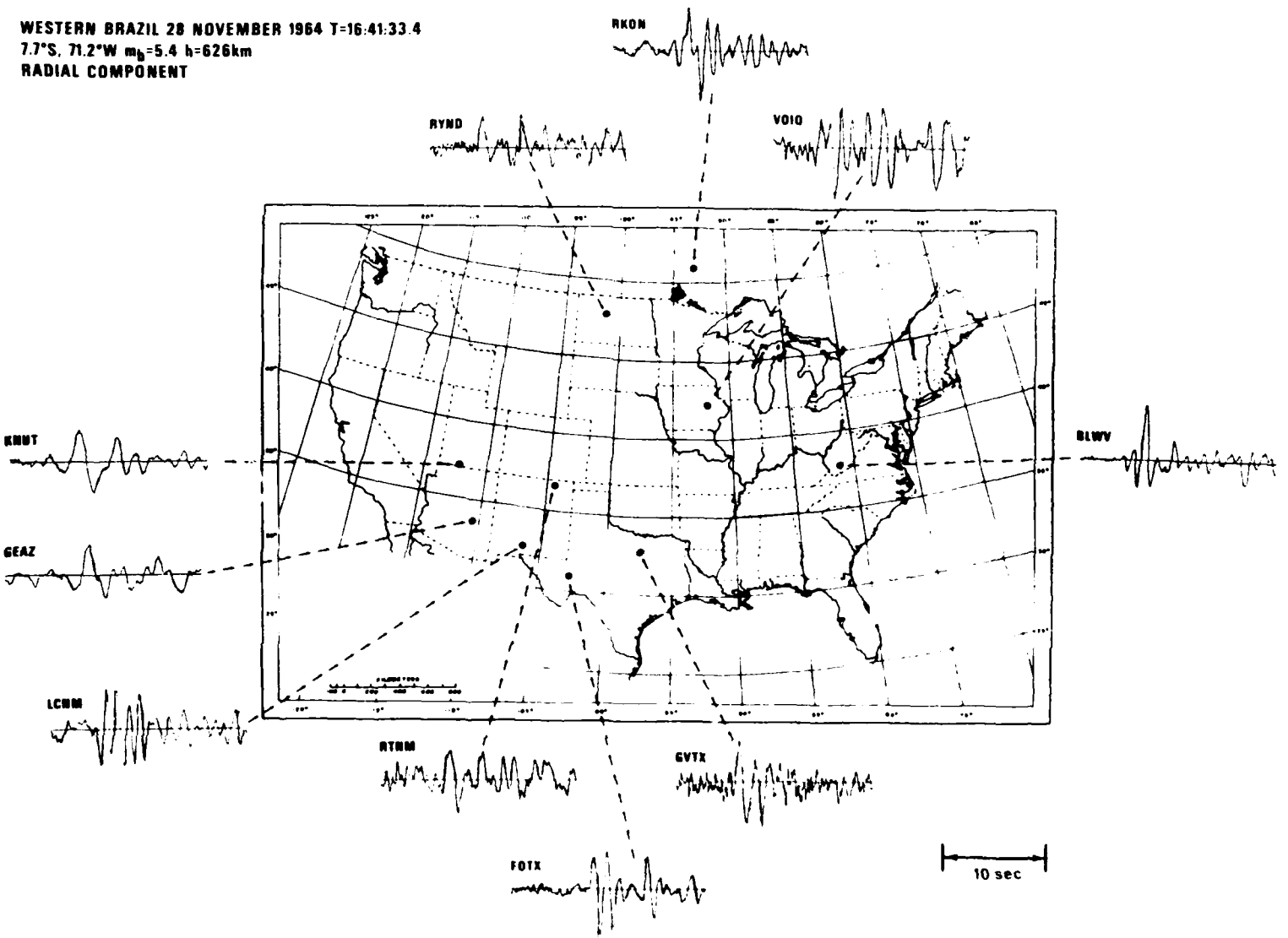

Figure 5. Radial component waveforms of short period S from the W. Brazil event at various LRSM stations.

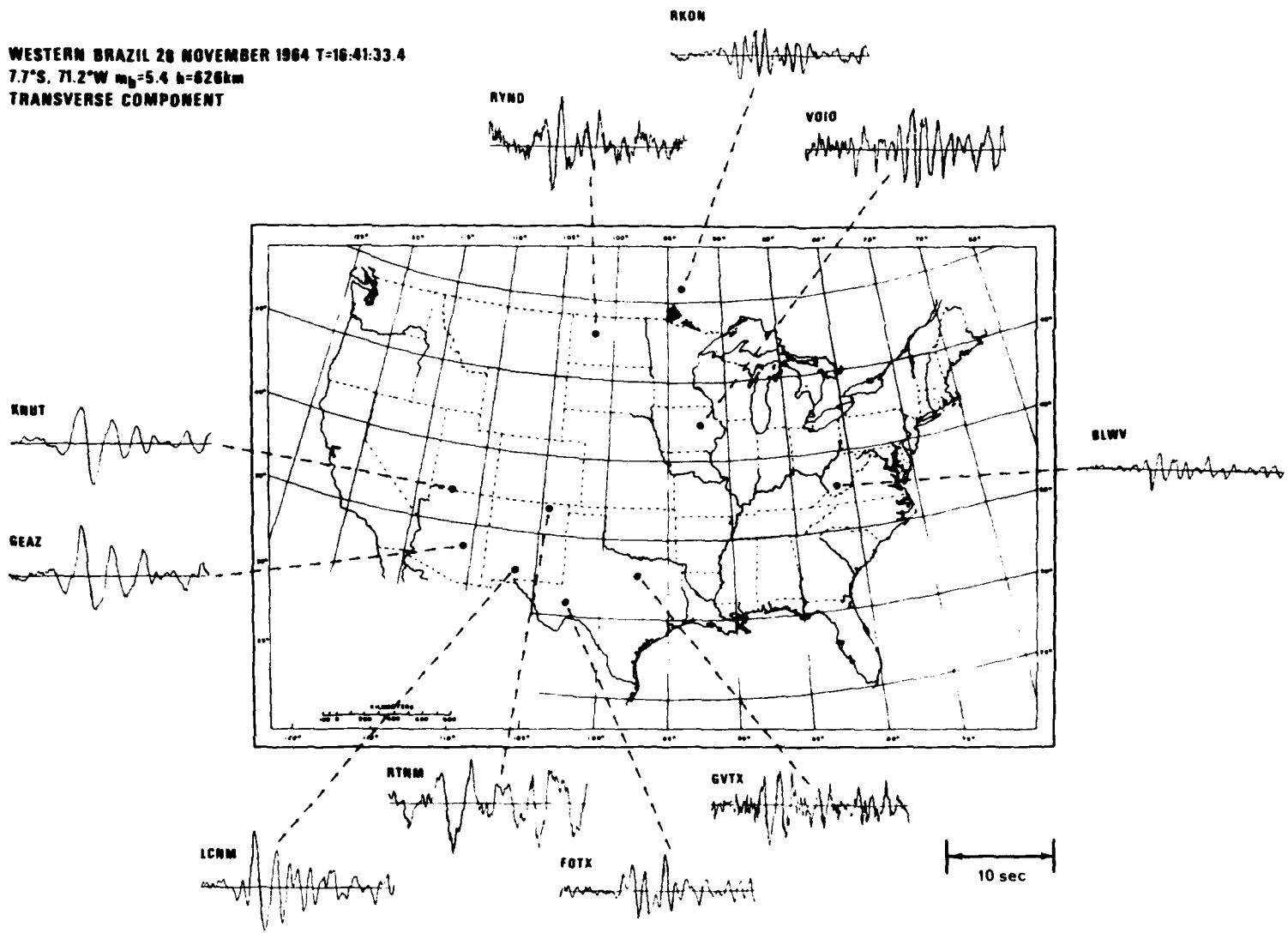

Figure 6. Transverse component waveforms of short period S from the W. Brazil event at various LRSM stations.

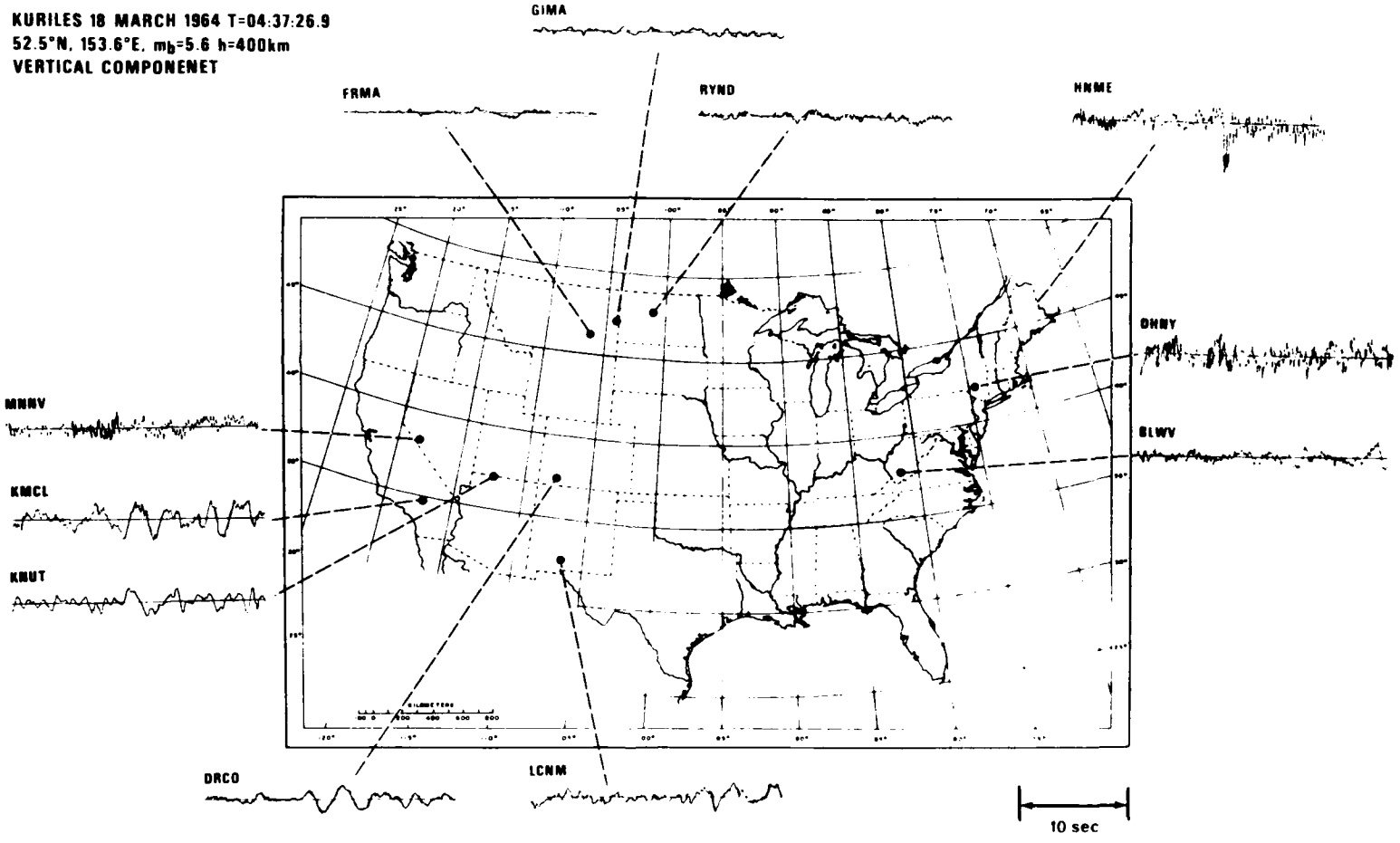

Figure 7. Vertical component waveforms of short period S from the Kurile Islands event at various LRSM stations.

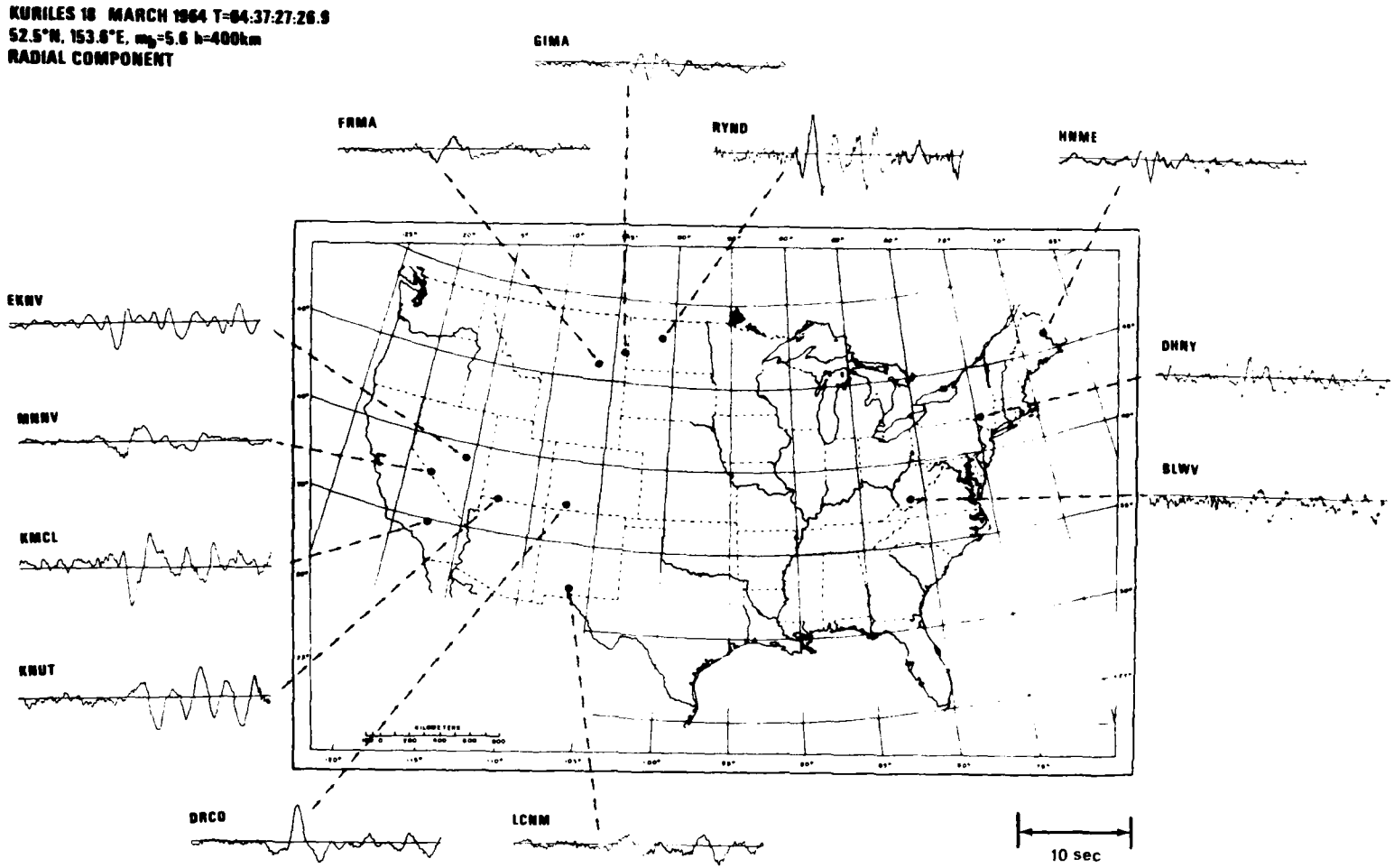

Figure 8. Radial component waveforms of short period S from the Kurile Islands event at various LRSM stations.

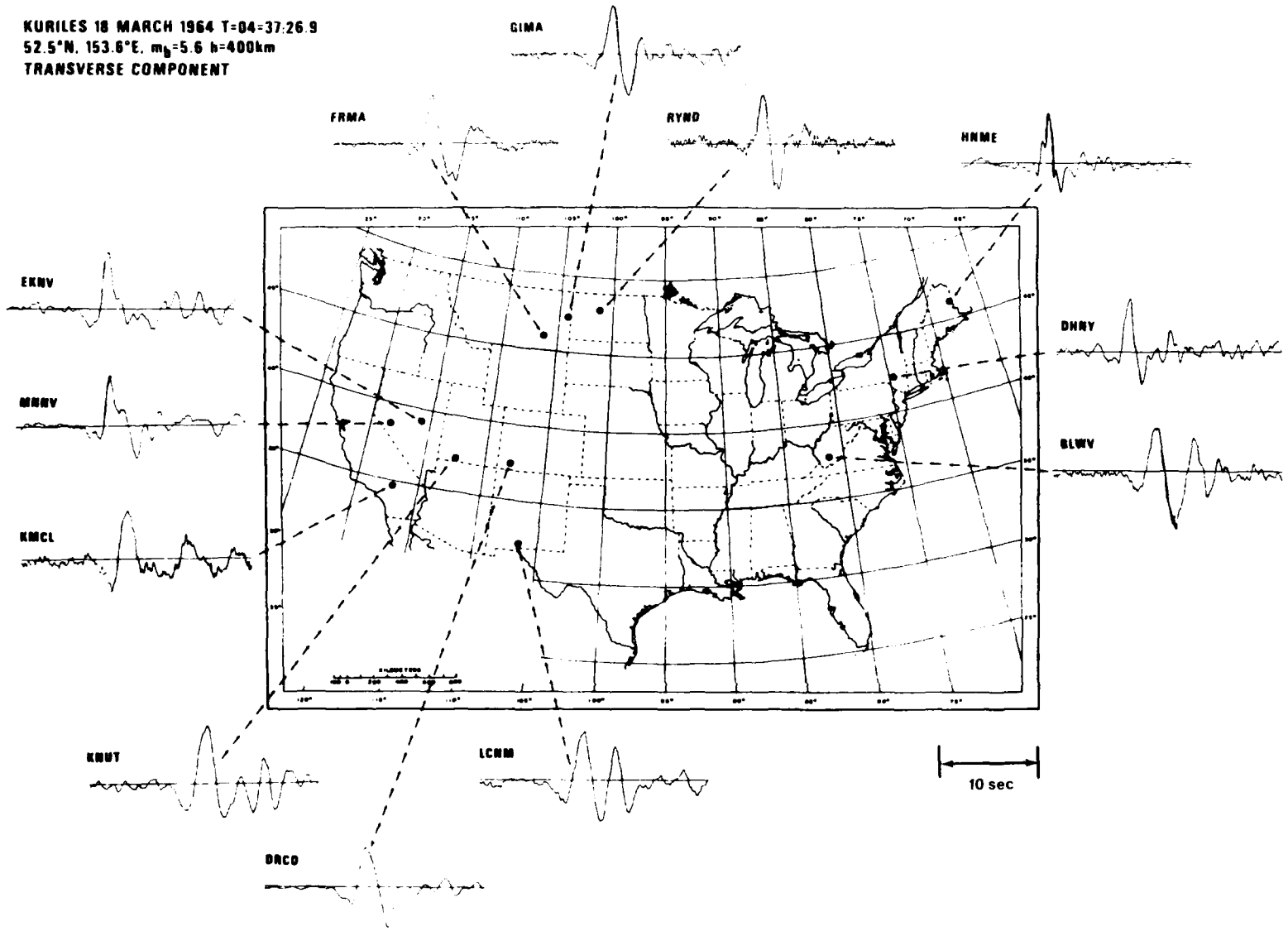

Figure 9. Transverse component waveforms of short period S from the Kurile Islands event at various LRSM stations.

at stations in the shield "core" of the continent: AYSD, SEMN and HTMN. High frequencies are absent at MVCL, MNNV, HLID, TFCL, KNUT, DRCO and DPCL. (The high frequency riding on some of these waveforms is clearly noise background preceding the S arrival.) Note that for the Argentine event, of all the WUS stations, DRCO and KNUT have the shortest dominant S wave period, which may indicate somewhat less attenuation under the Colorado Plateau (Der and McElfresh, 1977) than in the rest of the WUS. Another curious feature of these figures is the longer period waveforms at the northeastern stations, DHNY, TUPA and BLWV. This feature lends some credibility to Solomon and Toksöz's (1970), assertion that lower Q exists in the mantle under the northeastern United States.

Waveforms from the event in western Brazil (Figures 4 to 6) confirm the picture drawn from waveforms of the Argentine event, except for the waveform of the LCNM station which exhibits a high frequency character.

Although, the S pulses are generally shorter in the east (with the exception of BLWV), the waveforms from the Kurile Islands events (Figures 7 to 9) are less diagnostic. Apparently, the source of this earthquake radiated very little energy at high frequencies.

The regional S wave data seem to agree with the following quantitative gradation of the upper mantle Q under the United States:

a) Extremely high Q - Canadian Shield and adjoining regions in the US (AYSD, SEMN, HTMN, RKON, VOIO, RYND).
b) High Q - The rest of EUS with the exception of NEUS (Northeastern US).
c) Moderate Q - NEUS.
d) Low Q - WUS

Other types of geophysical data seem to agree well with this picture (heat flow, conductivity, P attenuation, P_n velocities, etc.). A possibly lower Q NEUS, however, is difficult to explain and considerably more research is needed before such a fine lateral subdivision of Q variation (except WUS-EUS) is confirmed. In addition to existing spectral evidence for lower Q in the WUS, the amplitudes of S waves analyzed in this report are also lower in the WUS. Because this aspect of this data set has been previously evaluated by

Der et al., 1975 the amplitudes will not be discussed in this report. The dat sented here would not be sufficient to establish a magnitude bias foı ıves with any accuracy unless crustal and source radiation effects on S amplitudes were calculated and removed.

The power spectra of the waveforms shown are given in Figures 10 and 17. The slopes fitted are also drawn in the figures. Tables of spectral slopes (Tables II to VII) and resulting t* differences show the same regional patterns obtained from visual inspection of traces. Due to the low wave amplitudes on the vertical component, only the radial and transverse components were used in our analysis. The Argentine event had the broadest source spectrum, extending to high frequencies, and the associated measurements of t* were considered the most reliable of the events studied here. Source spectra of the western Brazil and Kurile Islands events were confined more to low frequencies and, therefore, because fewer points were available to fit the spectral slopes, the calculated t* values were less reliable.

The spectral slopes of the transverse components from the Argentine event constitute two non-overlapping populations when grouped according to station locations in the WUS and EUS, respectively. The populations of spectral slopes from radial components have one overlapping value. Because of this situation, the difference in spectral slopes and regional t* averages are highly significant for the Argentine event. Strictly speaking, because differences in individual station t* can also play a role, the spread of values in each population is not solely a result of experimental error. The authors' past experience with spectral ratios (Der et al., 1977) showed that most scatter is due to the inherent uncertainty in the spectral fitting procedure.

The average value of the EUS-WUS t* differential found for short period S waves, $\Delta t^*_s \sim .67 \pm .19$, is several times greater than the corresponding regional differential for short-period P, Δt^*_s should be four times Δt^*_p for losses in shear deformation only. The present data cannot rule out this value, but $\Delta t^*_s = \Delta t^*_p$ can be ruled out. Thus, our results do not conflict with the assertion that for short-period body waves most - if not all - anelastic energy loss occurs in shear deformation.

ARGENTINA, 29 Sep 62 O.T.=1517:47.7Z

h=575km 27.0°S 63.6°W m_b=6.5

WESTERN U.S., RADIAL COMPONENT

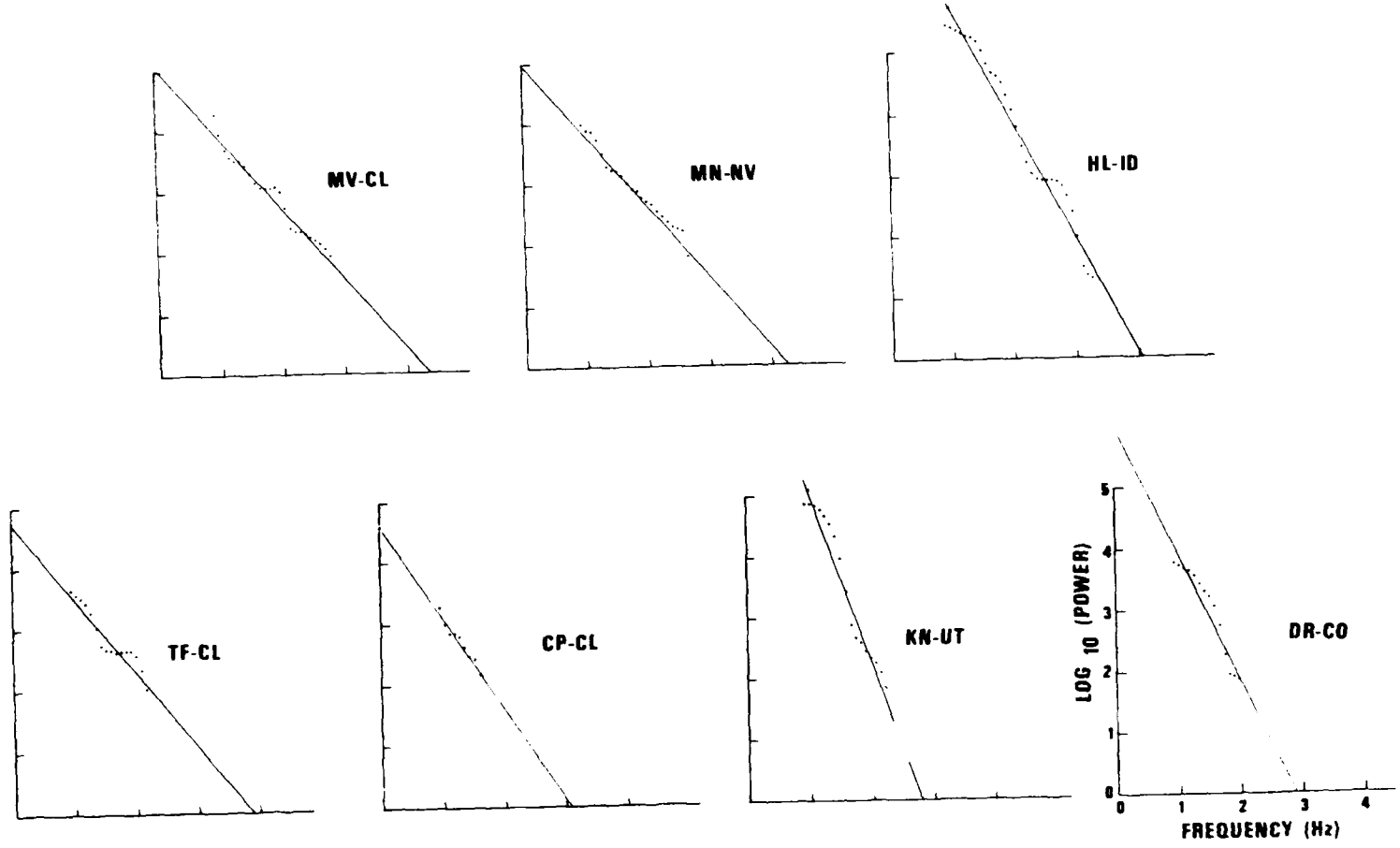

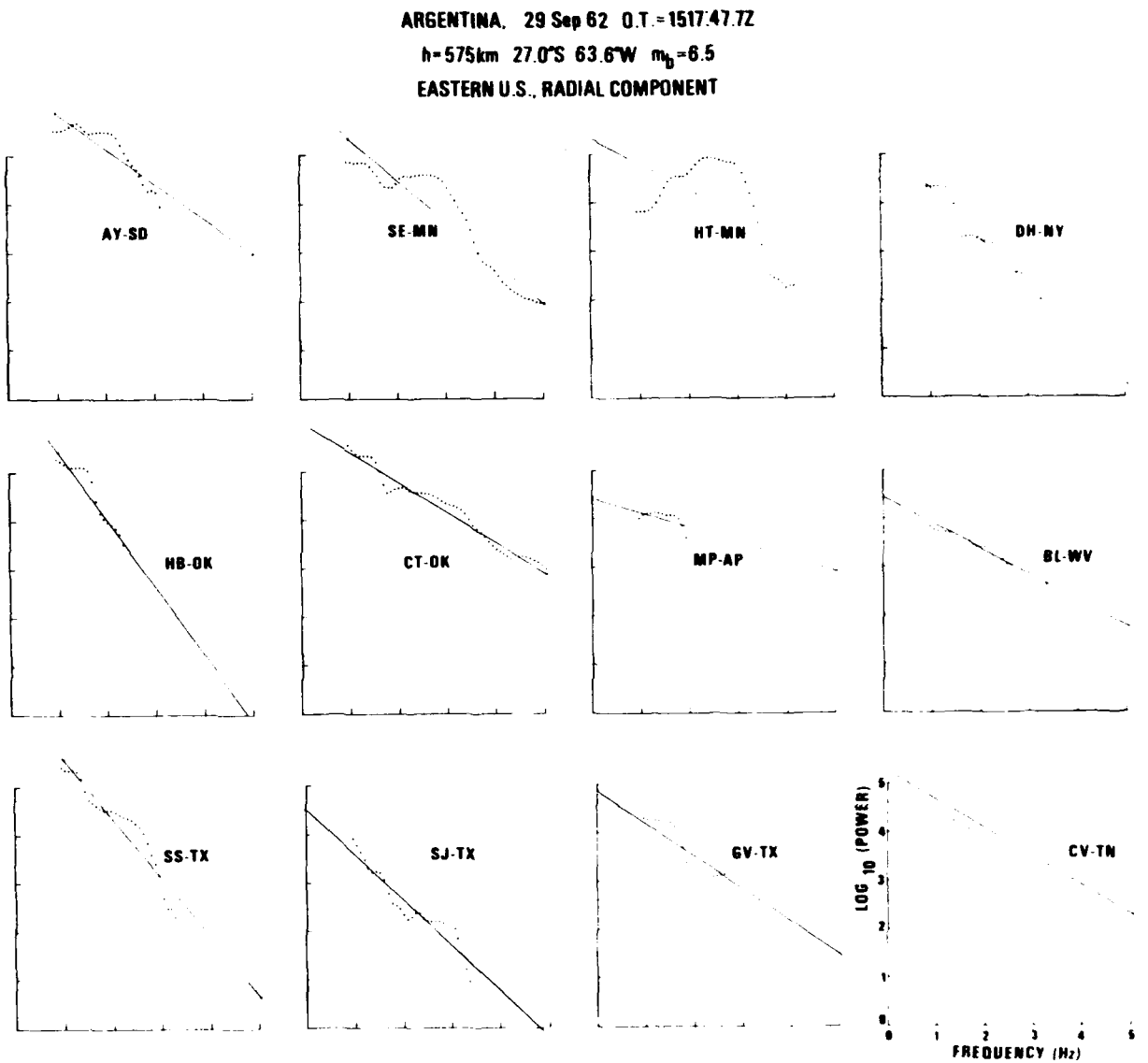

Figure 11. Power spectra of the radial component of short period S at various LRSM stations, Argentine event.

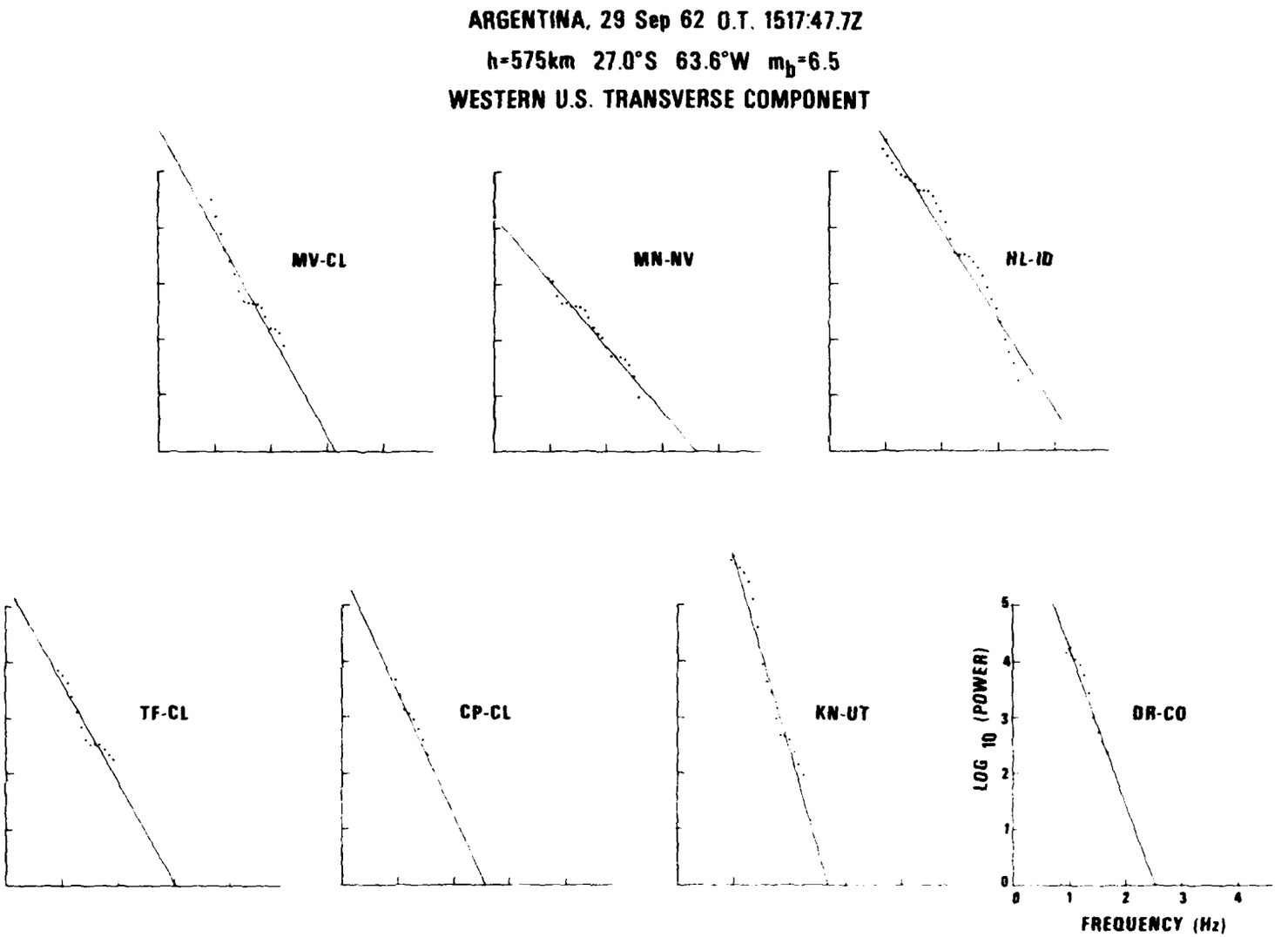

Figure 12. Power spectra of the transverse component of short period *S at various LRSM stations*, Argentine event.

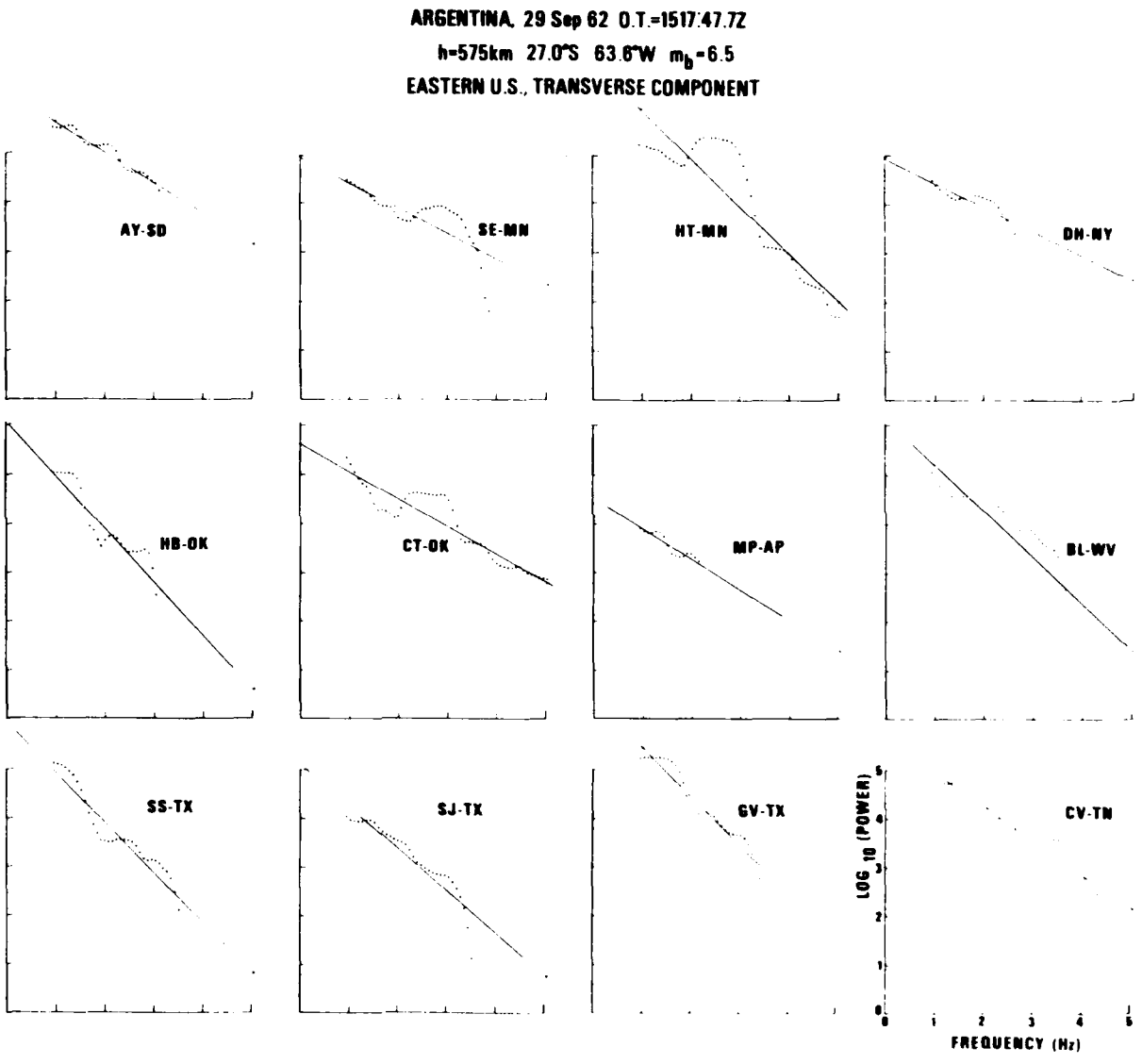

Figure 13. Power spectra of the transverse component of short period S at various LRSM stations, Argentine event.

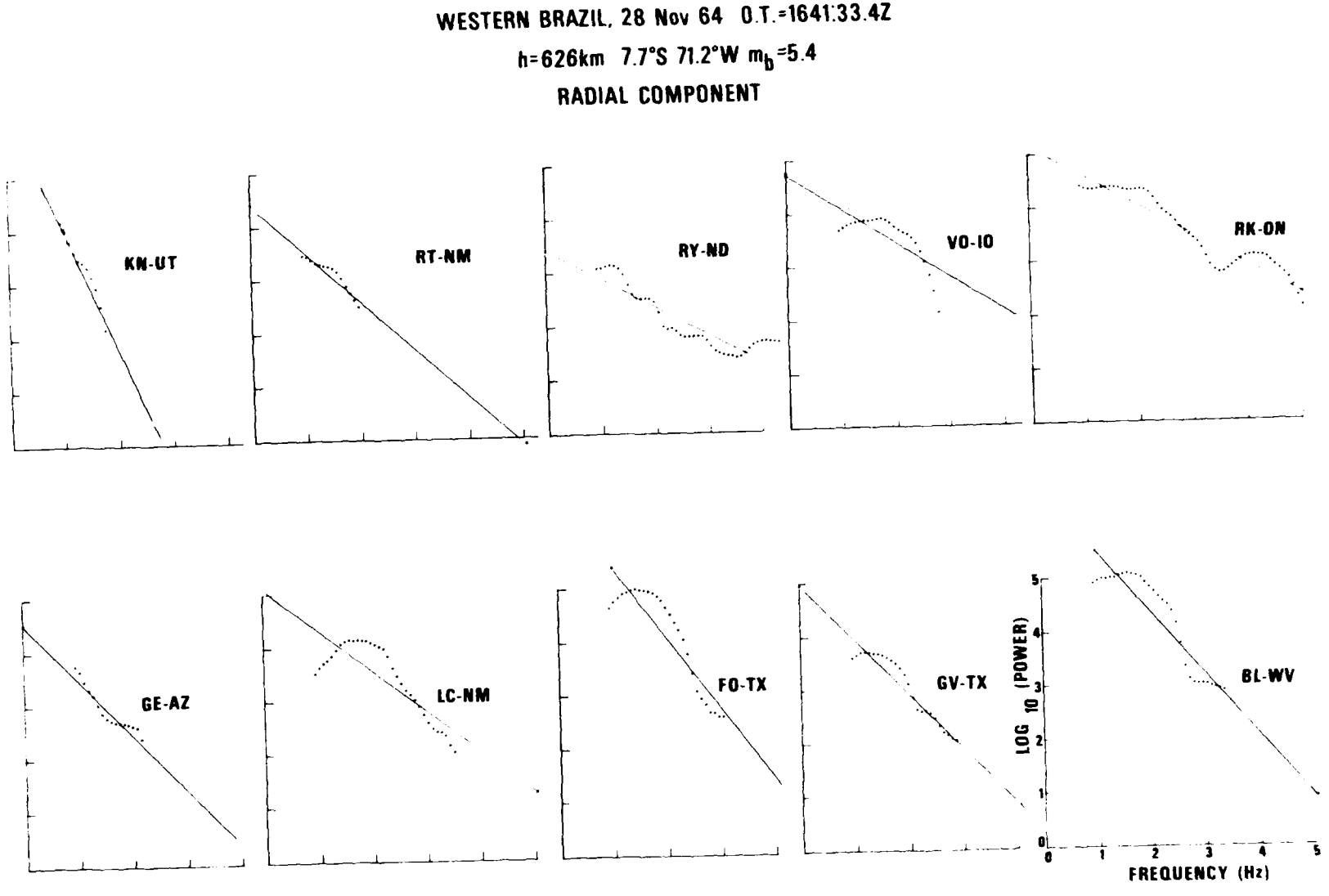

Figure 14. Power spectra of the radial component of short period S at various LRSM stations, W. Brazil event.

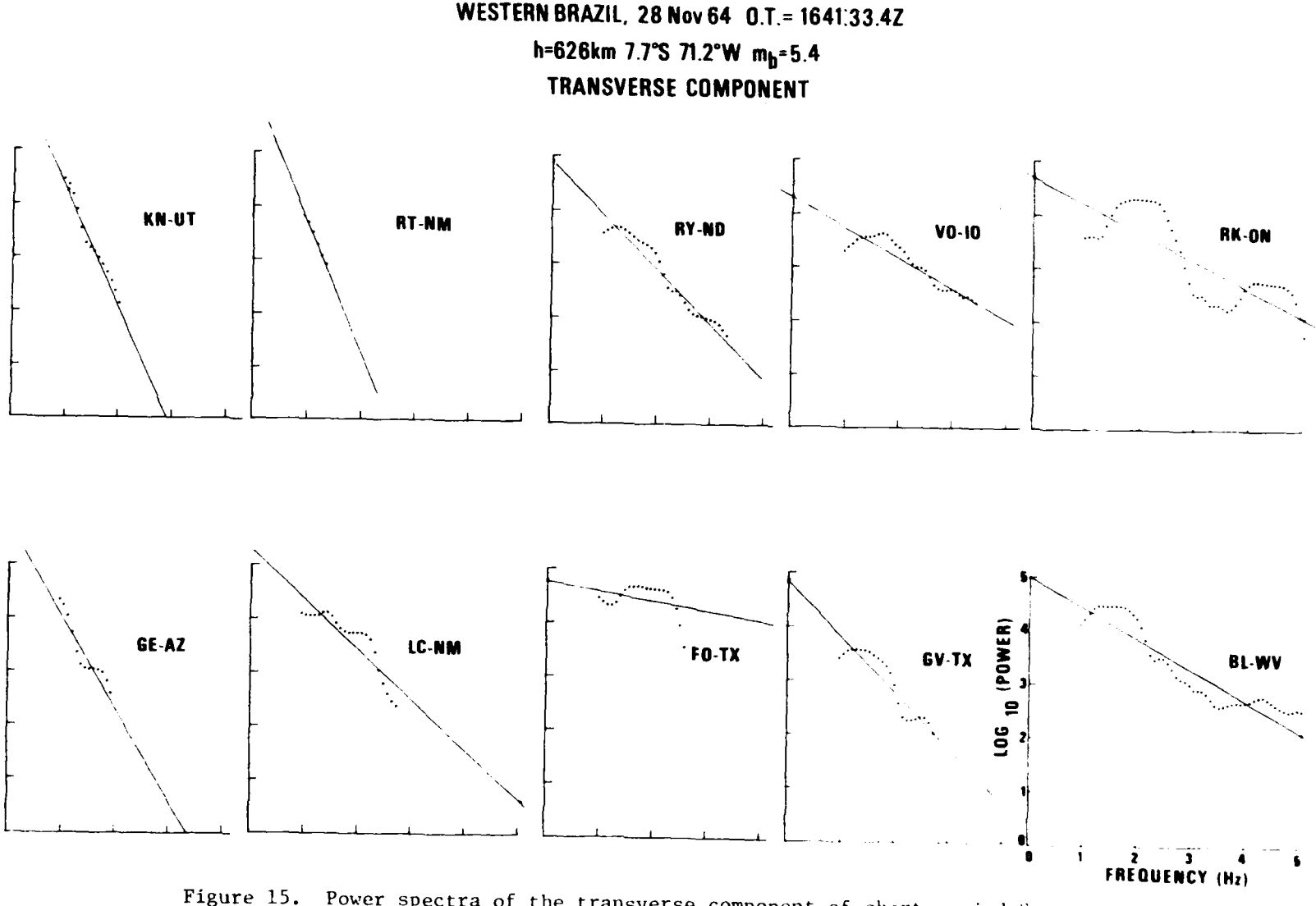

Figure 15. Power spectra of the transverse component of short period S at various LRSM stations, W. Brazil event.

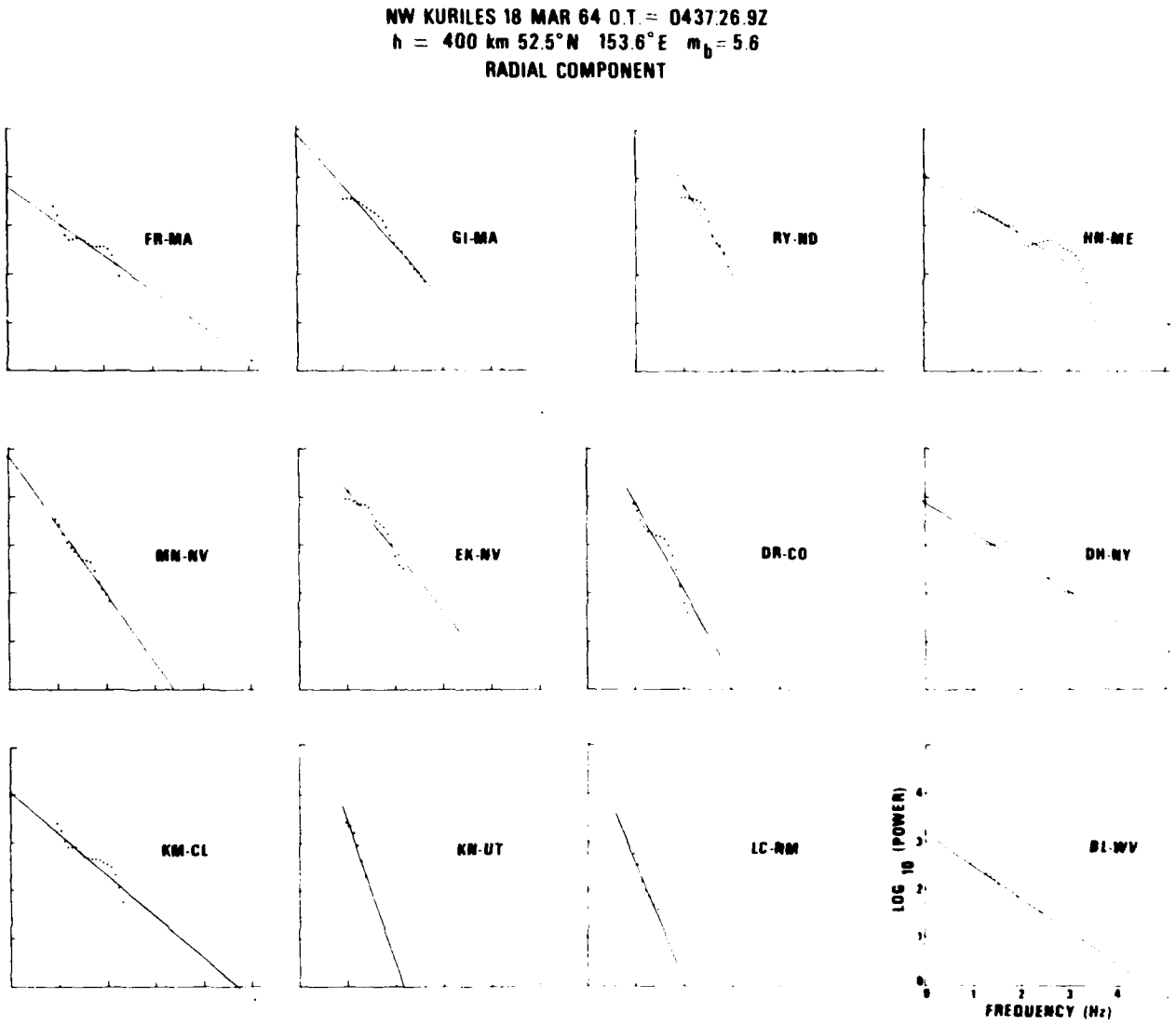

Figure 16. Power spectra of the radial component of short period S at various LRSM stations, Kurile Islands event.

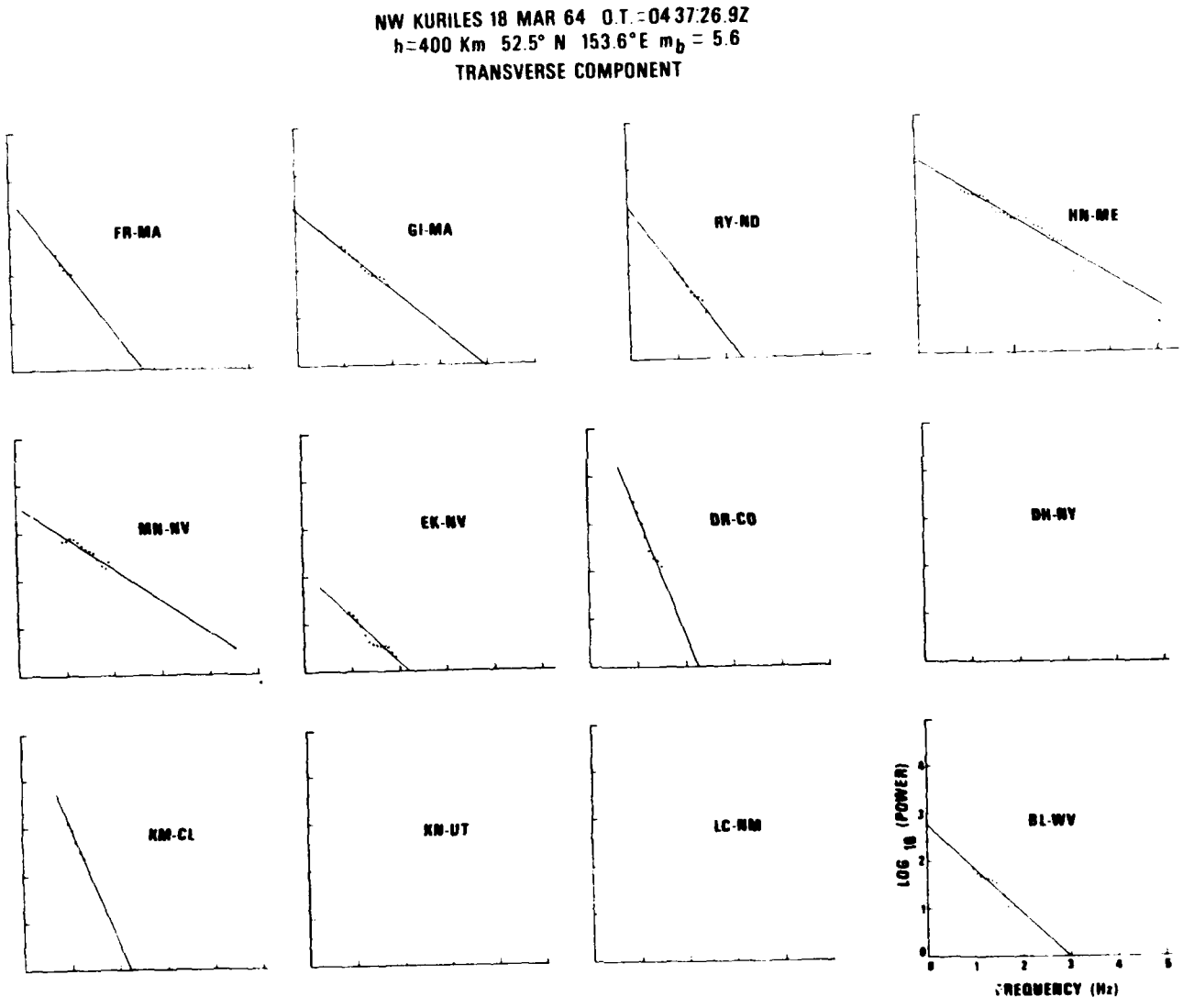

Figure 17. Power spectra of the transverse component of short period S at various LRSM stations, Kurile Islands event.

The fact that short-period S waves exhibit regional spectral differences, which are similar to those of short-period P, strengthens the interpretation of the WUS magnitude anomaly as a regional anelastic attenuation effect. It would be impossible to explain the observations with crustal structure or scattering.

Observed Regional t_s^* Variations and Focal Mechanisms

The focal mechanism of faulting with finite length may also affect the spectra of radiated waves. For example, azimuthal dependence in spectra may by introduced by a Doppler shift along a unilaterally propagating fault. The maximum Doppler effect will lie along one of the P-wave nodal planes and die away as the cosine of the angular distance on the focal sphere. There is information available on the focal mechanism of the events used in our regional analysis. Mediguren (1969) discussed the focal mechanisms of a group of deep Argentine events, including the event used in this report. If the US stations are plotted on the composite focal mechanism diagram of Mendiguren (Figure 18), all these stations fall on the node of the P wave radiation pattern where the Doppler variation is minimum for S. (The notations used for various stations are given in Table VIII.) In any event the United States occupies only a very small portion of the focal sphere and it would be remarkable if differences across the US could be attributed to the source mechanism.

Berckhemer and Jacob (1968) and Veith (1974) have studied the Kurile event used in the sample. Veith's focal mechanism solution shows a P-wave nodal line across the northeastern US (Figure 19), but not coinciding with the EUS-WUS boundary nor in the same location as the fault plane for the Argentine event.

Mendiguren, J. A. (1969). Study of focal mechanism of deep earthquakes in Argentina using nonlinear particle motion of S waves, Bull. Seism. Soc. Am., 59, 1449-1473.

Berckhemer, H. and K. H. Jacob (1968). Investigation of the dynamical process in earthquake foci by analyzing the pulse shape of body waves, Final Scientific Report, Institute of Meteorology and Geophysics, University of Frankfurt, Germany. AD738953.

Veith, K. F. (1974). The relationship of island arc seismicity to plate tectonics, Ph.D. thesis, Southern Methodist University, Dallas, Texas.

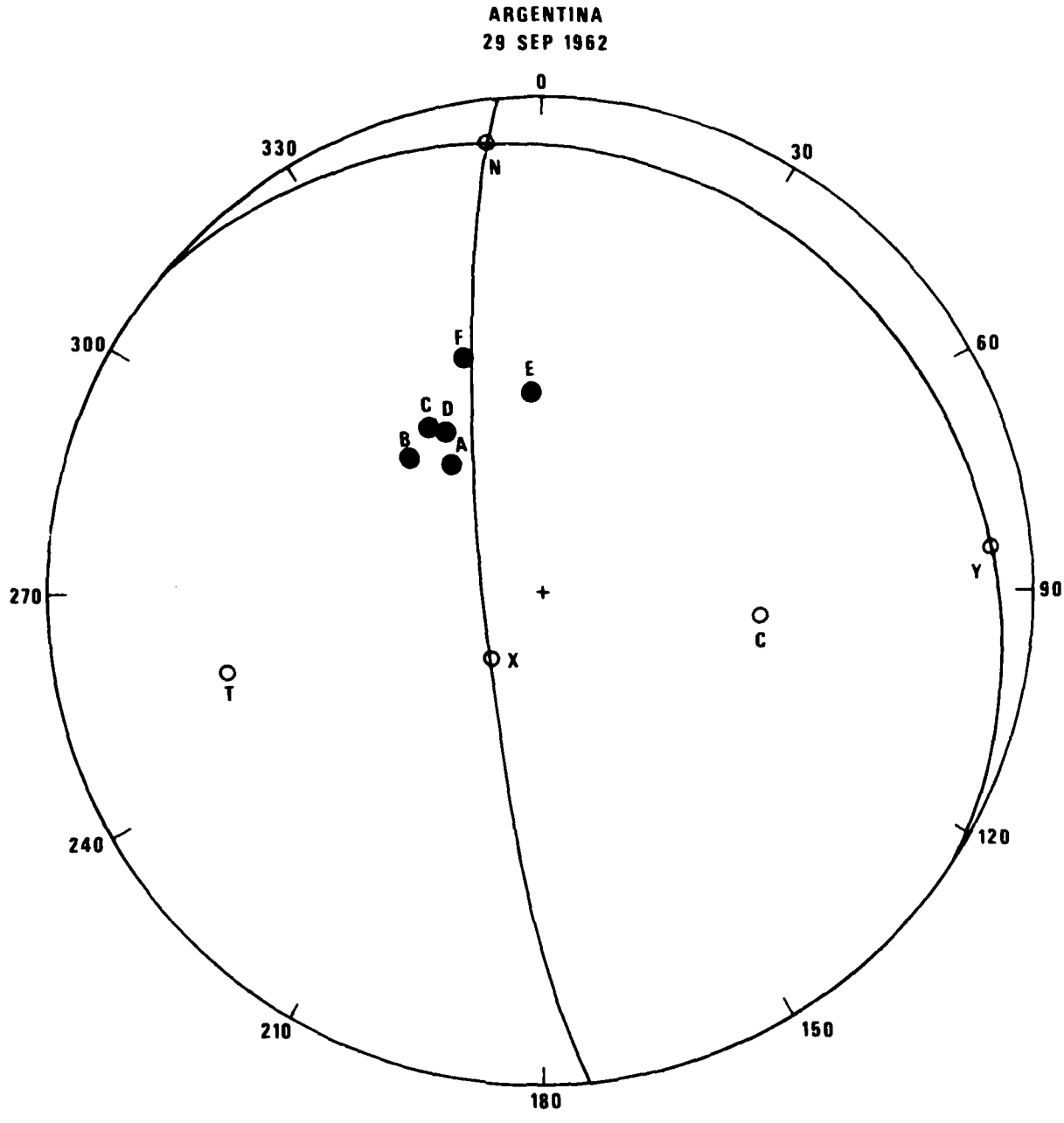

Figure 18. Composite focal mechanism of Argentine events with US stations superposed (after Mendiguren). Station designation is given in Table VIII.

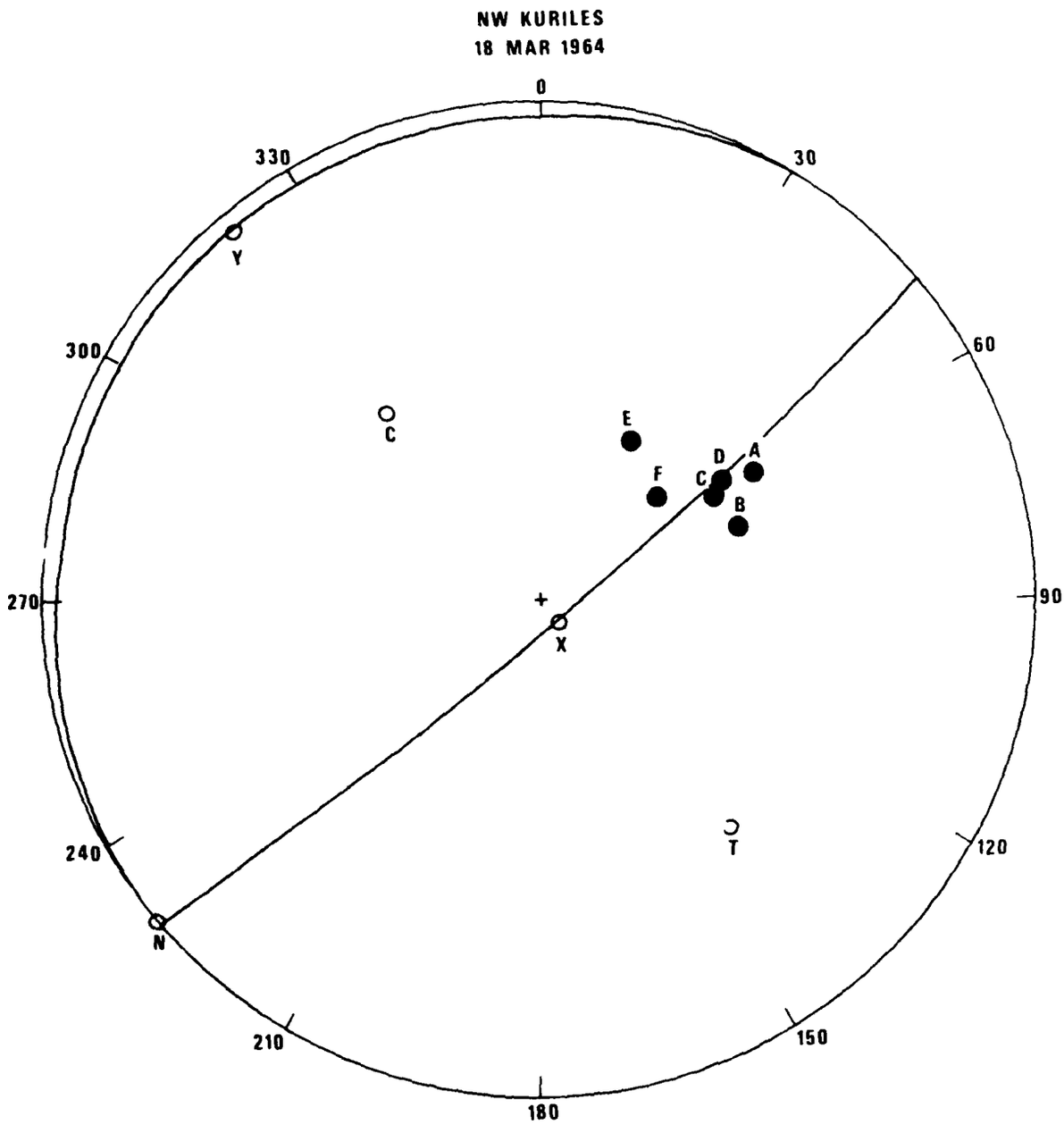

Figure 19. Focal mechanism of the Kurile event (after Veith) with US stations superposed. Station designation is given in Table VIII.

TABLE VIII

Explanation of Station Symbols in the Focal Mechanism Plots

Symbol	Station
A	MU-WA
B	CP-CL
C	RT-NM
D	PM-WY
E	HN-ME
F	BE-FL

Station Codes For Focal Diagrams

While the event in western Brazil does not have a published source mechanism, source mechanisms of many events in the same region have been studied. All of these are remarkably similar, with P-wave nodal lines running well outside the United States (Figures 20 and 21).

Figures 22 and 23 also show two fault plane solutions, derived by Berckhemer and Jacob (1968) from short-period recordings of P, which differed from those derived from long-period data. Berckhemer and Jacob interpreted this difference as a change of focal mechanism during the rupture process due to a reorientation of stress; none of the P-wave nodal lines of the two source mechanisms pass through the United States. Berckhemer and Jacob also studied in detail P wave pulse shapes of the Kurile and western Brazil events. They could not see any azimuthal variations in P wave shapes, suggesting that S wave shapes (as distinct from amplitudes) would also be insensitive to azimuth.

The data presented above demonstrates that spectral changes between WUS and EUS described in this report could not be attributed consistently to focal mechanisms for any of the events studied. S wave radiation patterns do affect the absolute amplitude levels significantly for some of our events, but can not be a factor in influencing the results of our t* study in any consistent manner.

Data From the NTS Experiment

During the operation of the Nevada Test Site (NTS) stations, the authors routinely searched for short-period S phases. However, only a few events were found where the quality of the S phases was acceptable for spectral analysis; these are listed in Table IX. The rotated traces, power spectra, and power spectral ratios for these events are shown in Figures 24 to 37. Because vertical components of motion were small, only radial and transverse components were used in the analysis. Tables X to XII summarize the slopes of spectral ratios and the associated Δt^*. The data show a behavior in agreement with the regional pattern outlined above. For the RKON/OB2NV pair, seven of the eight slopes of spectral ratios are positive, indicating less high frequency content of S waves at OB2NV. This result suggests higher anelastic attenuation under OB2NV than under RKON, a finding in agreement with the P wave spectral

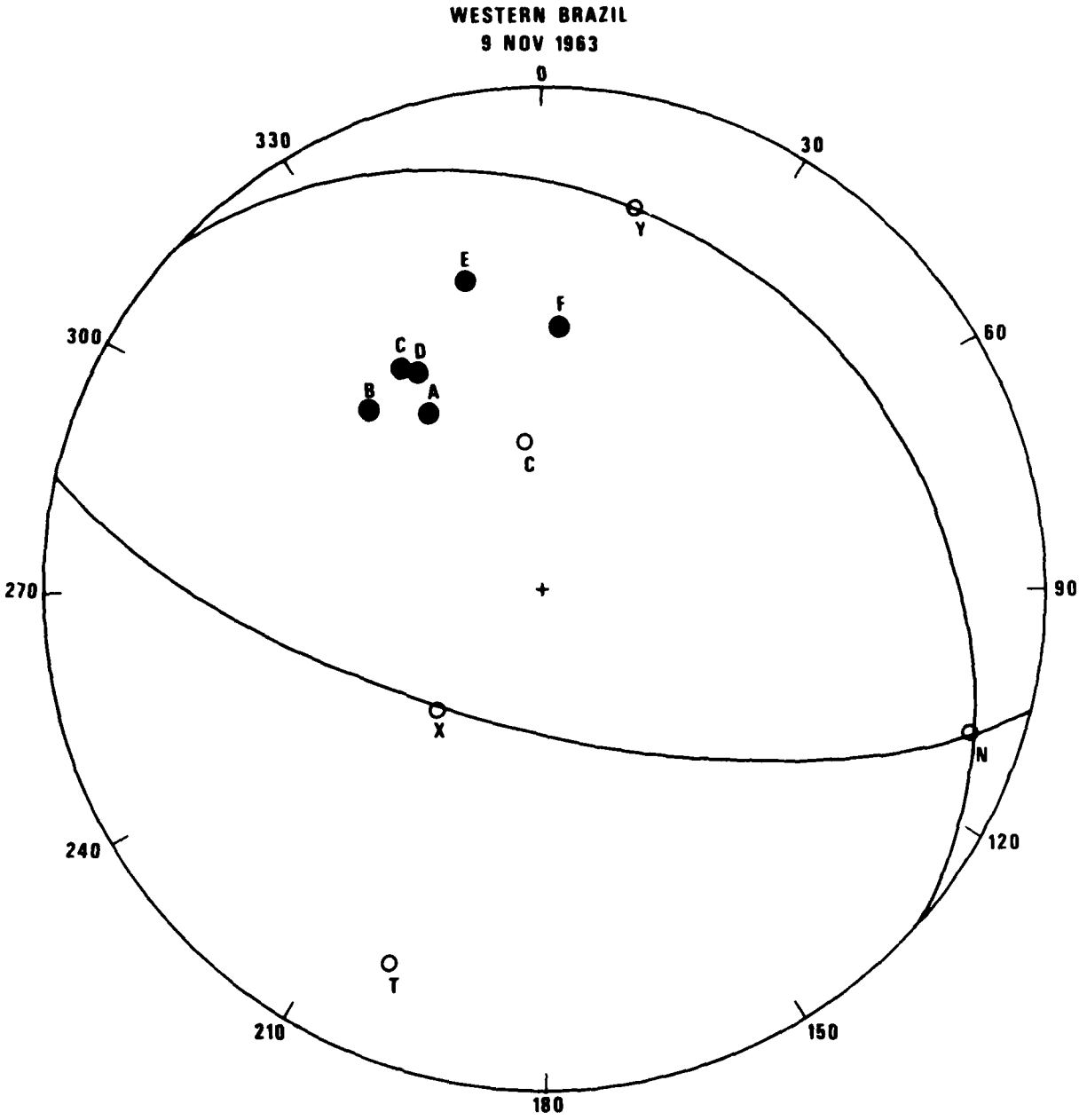

Figure 20. Focal mechanism of a 9 Nov 1963 W. Brazil event with US stations superposed. Station designation is given in Table VIII.

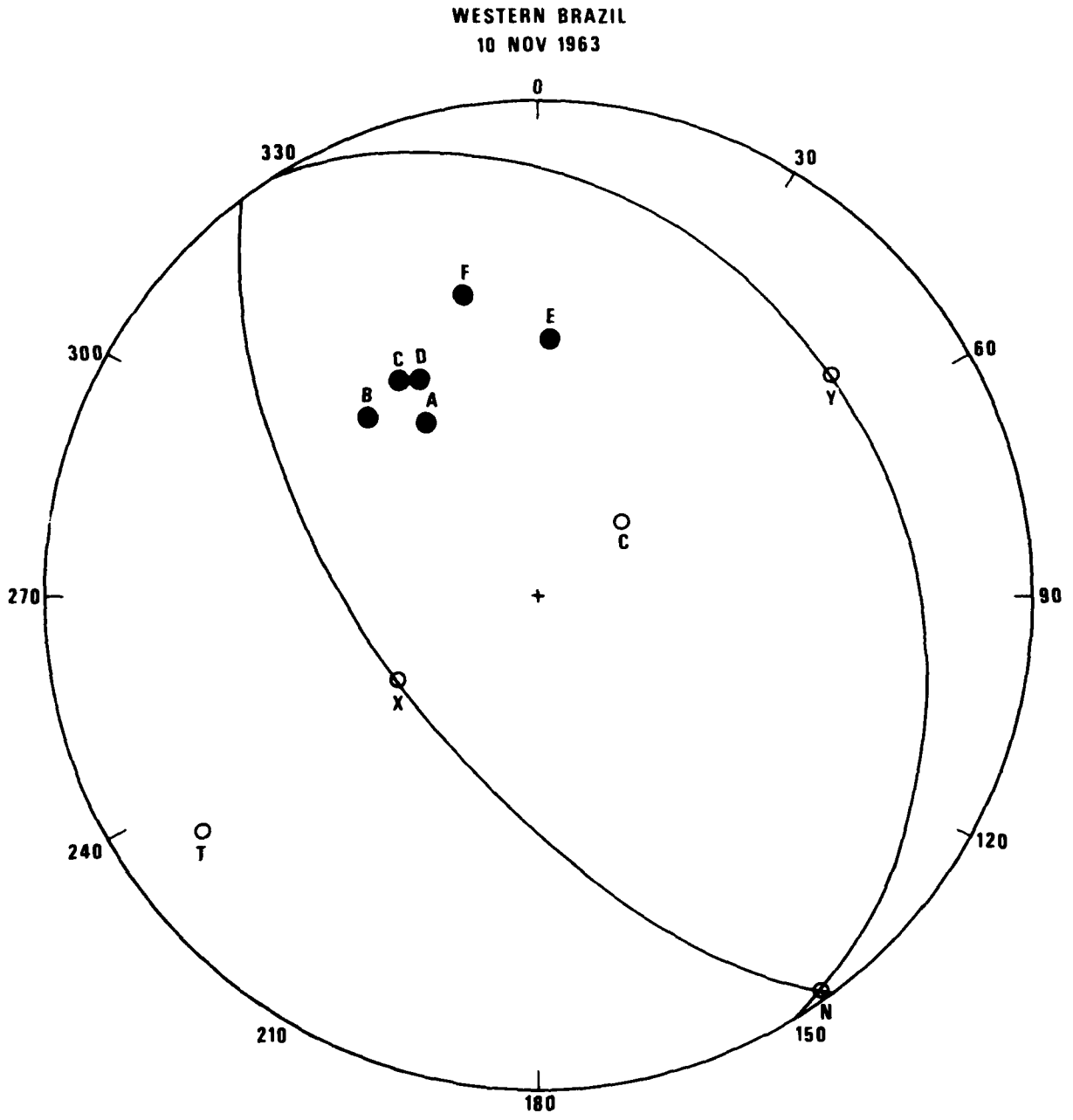

Figure 21. Focal mechanism of a 10 Nov 1963 W. Brazil event with US stations superposed. Station designation is given in Table VIII.

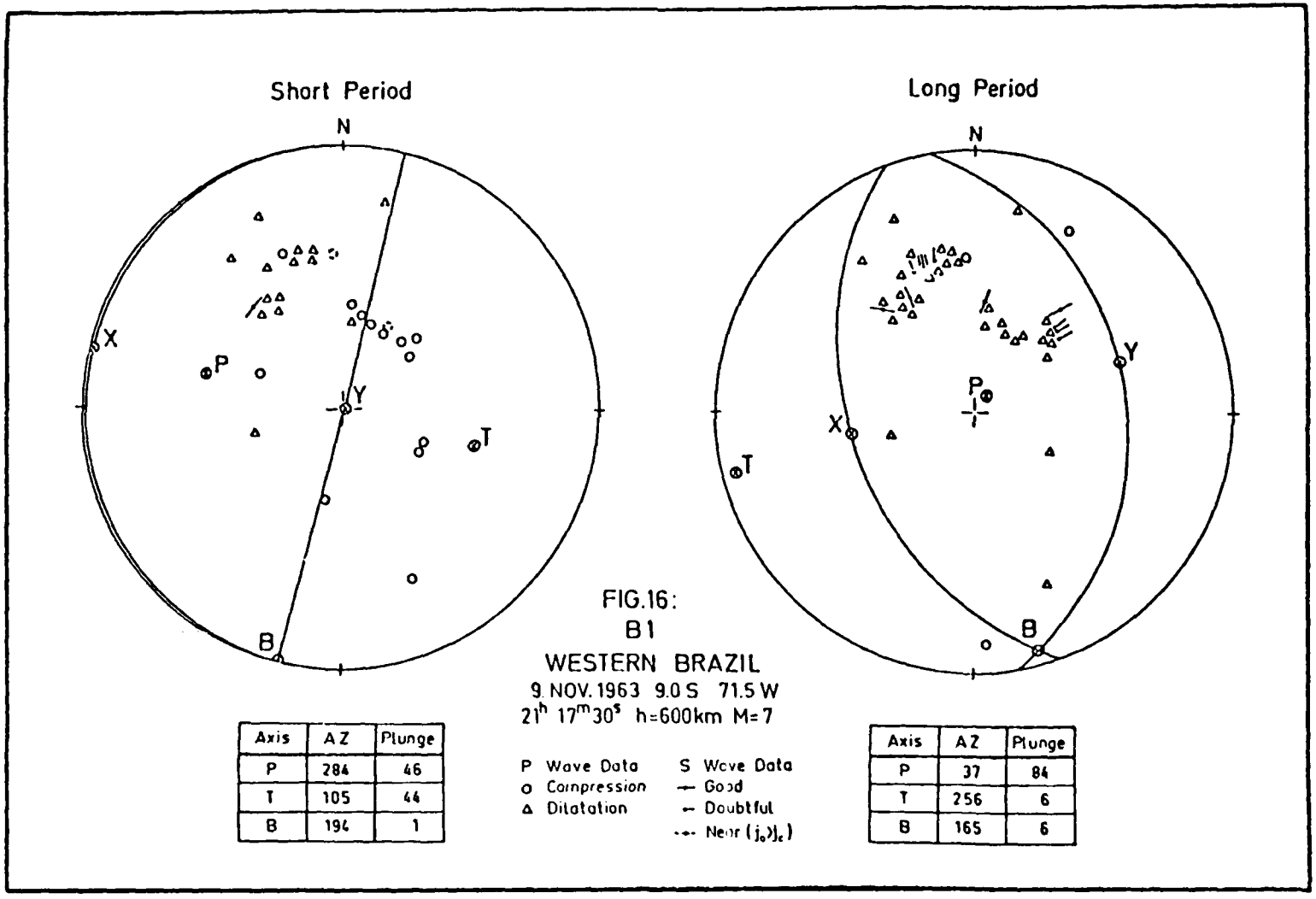

Axis	AZ	Plunge
P	284	46
T	105	44
B	194	1

Axis	AZ	Plunge
P	37	84
T	256	6
B	165	6

Figure 22. Short and long period focal mechanisms of the 9 Nov 1963 W. Brazil event (after Berckhemer and Jacob, 1968).

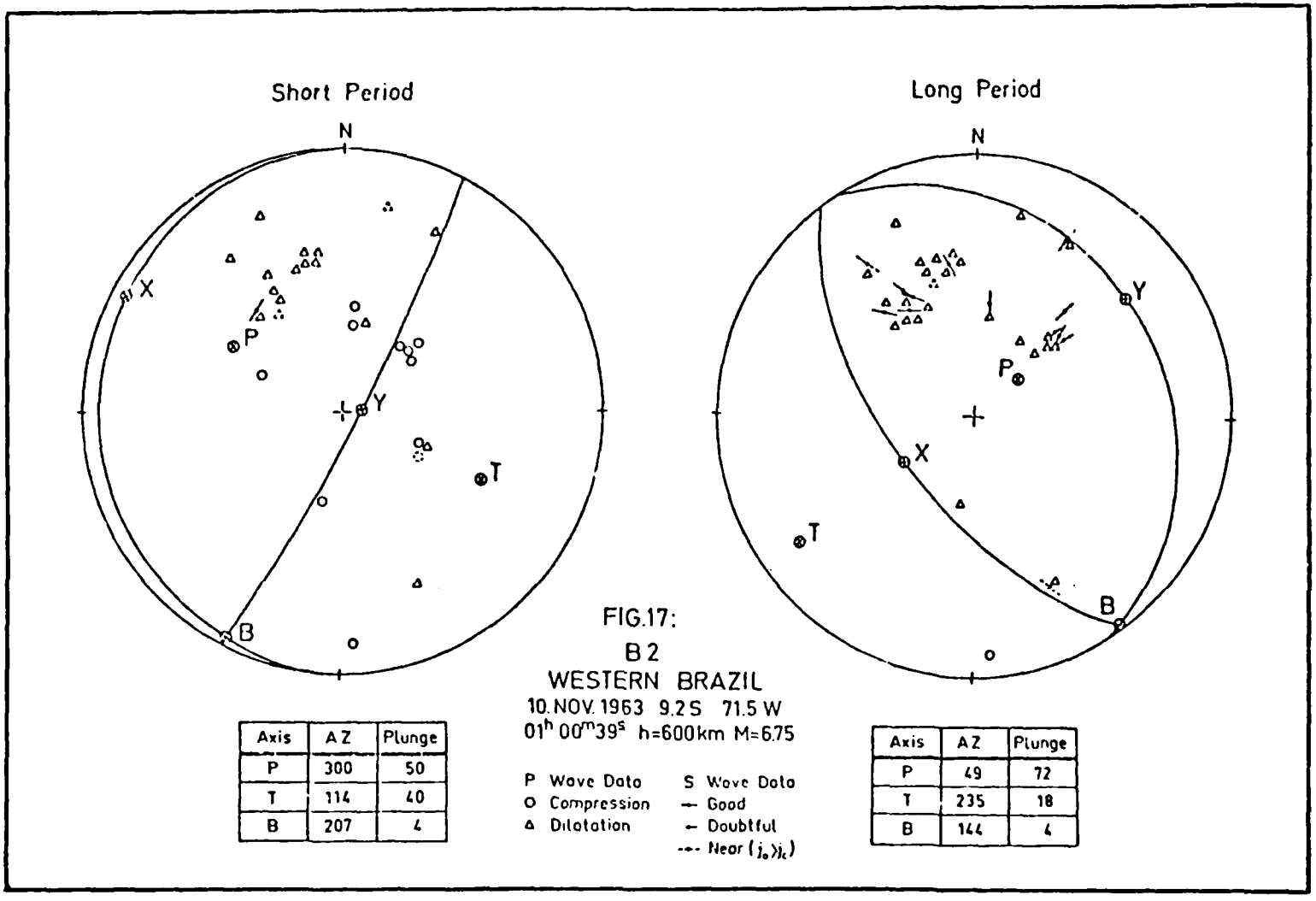

Axis	AZ	Plunge
P	300	50
T	114	40
B	207	4

Axis	AZ	Plunge
P	49	72
T	235	18
B	144	4

Figure 23. Short and long period focal mechanisms of the 10 Nov 1963 W. Brazil event (after Berckhemer and Jacob, 1968).

TABLE IX

Epicentral data of events used at SDCS stations.

Date	Origin Time	Coordinates	Geographical Region	Depth
17 Jun 77	02:29:22.3	19.7S, 179.2W	Fiji Islands Region	774
19 Jun 77	11:47:22.3	47.2N, 151.0E	Kurile Islands Region	118
24 Jun 77	19:55:38.9	19.4N, 144.9E	Mariana Islands	438
4 Sep 77	15:40:59.7	51.0N, 178.4E	Rat Islands, Aleu.	43
4 Sep 77	23:20:48.0	51.0N, 178.5E	Rat Islands, Aleu.	54
21 Apr 77	01:45:46.9	26.7N, 142.6E	Bonin Islands Region	0

April 21 ~ 02:00

Arrives 02:08

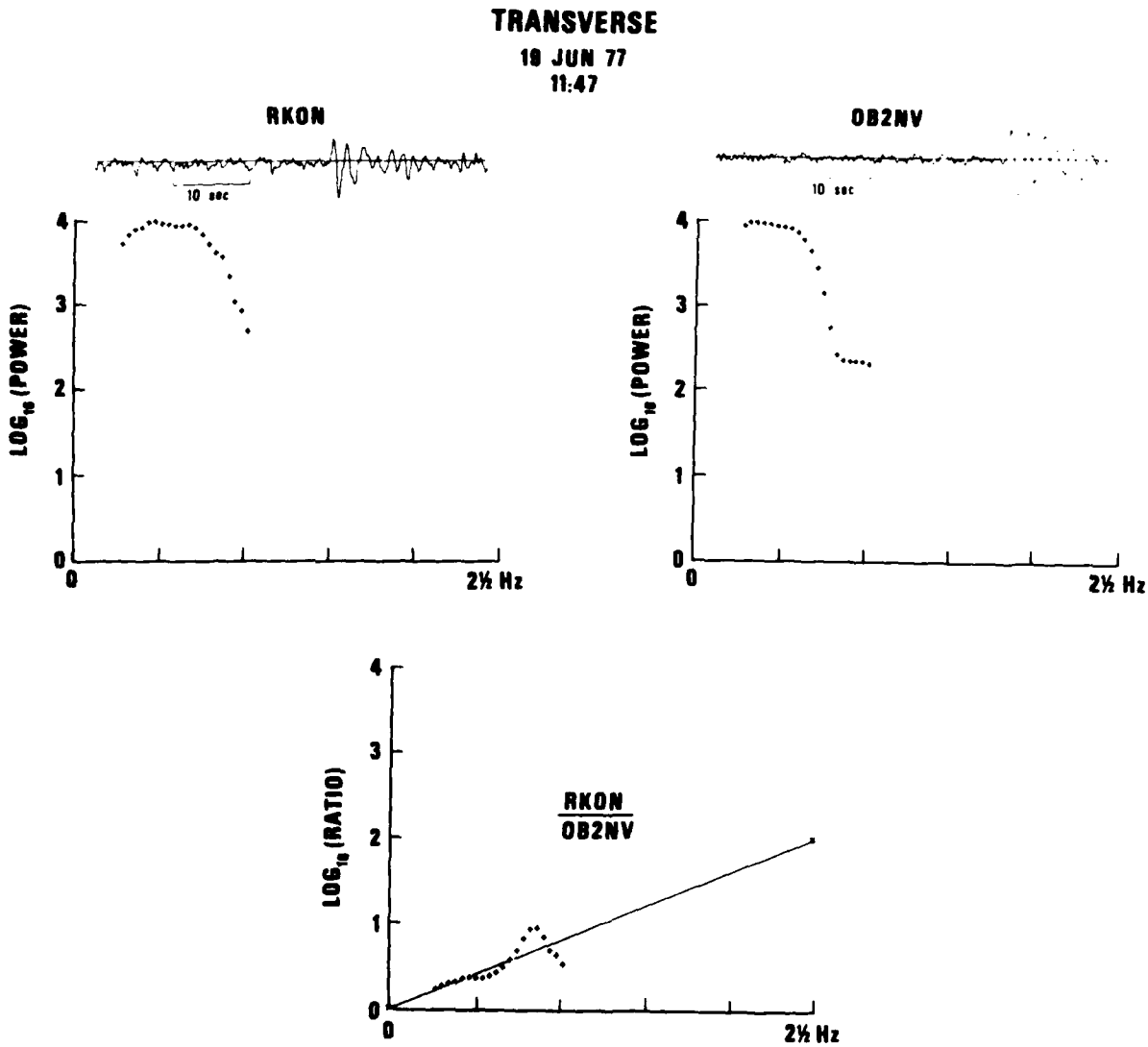

Figure 24. Time traces, power spectra and power spectral ratios for short period S waves observed at SDCS stations RKON and OB2NV, 19 June 1977 event, transverse component.

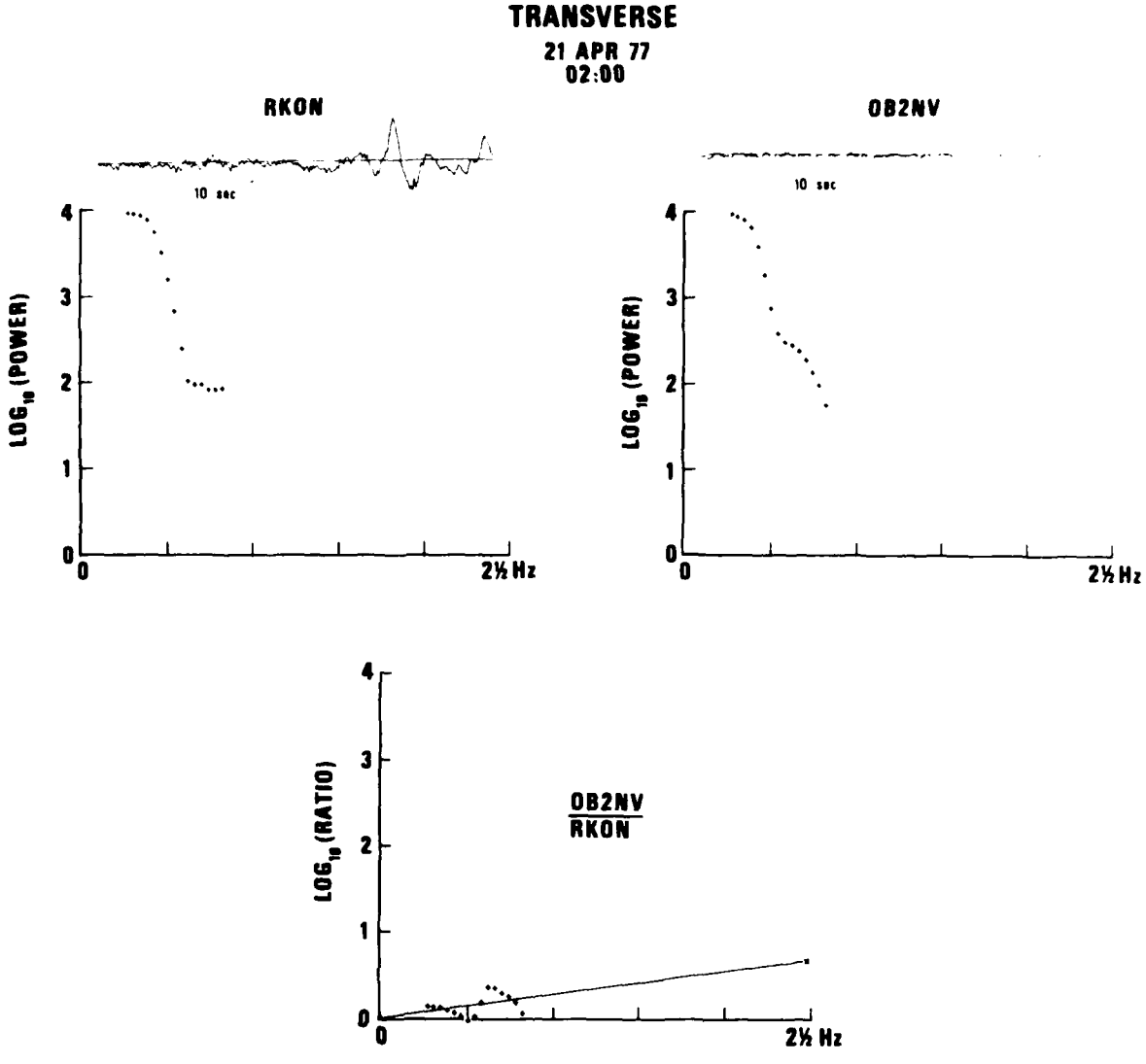

Figure 25. Time traces, power spectra and power spectral ratios for short period S waves observed at SDCS stations RKON and OB2NV, 21 April 1977 event, transverse component.

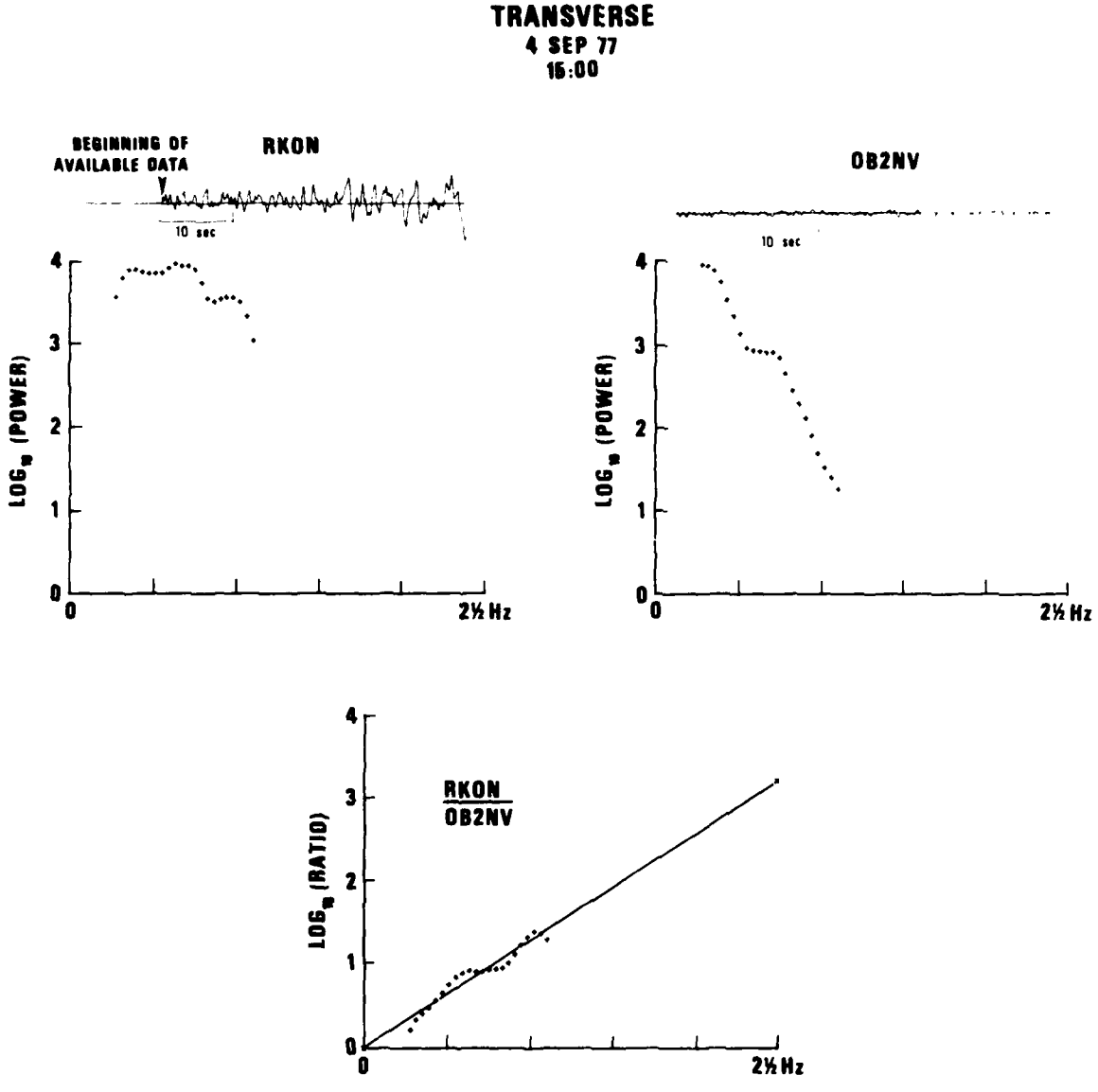

Figure 26. Time traces, power spectra and power spectral ratios for short period S waves observed at SDCS stations RKON and OB2NV, 4 September 1977 event, transverse component.

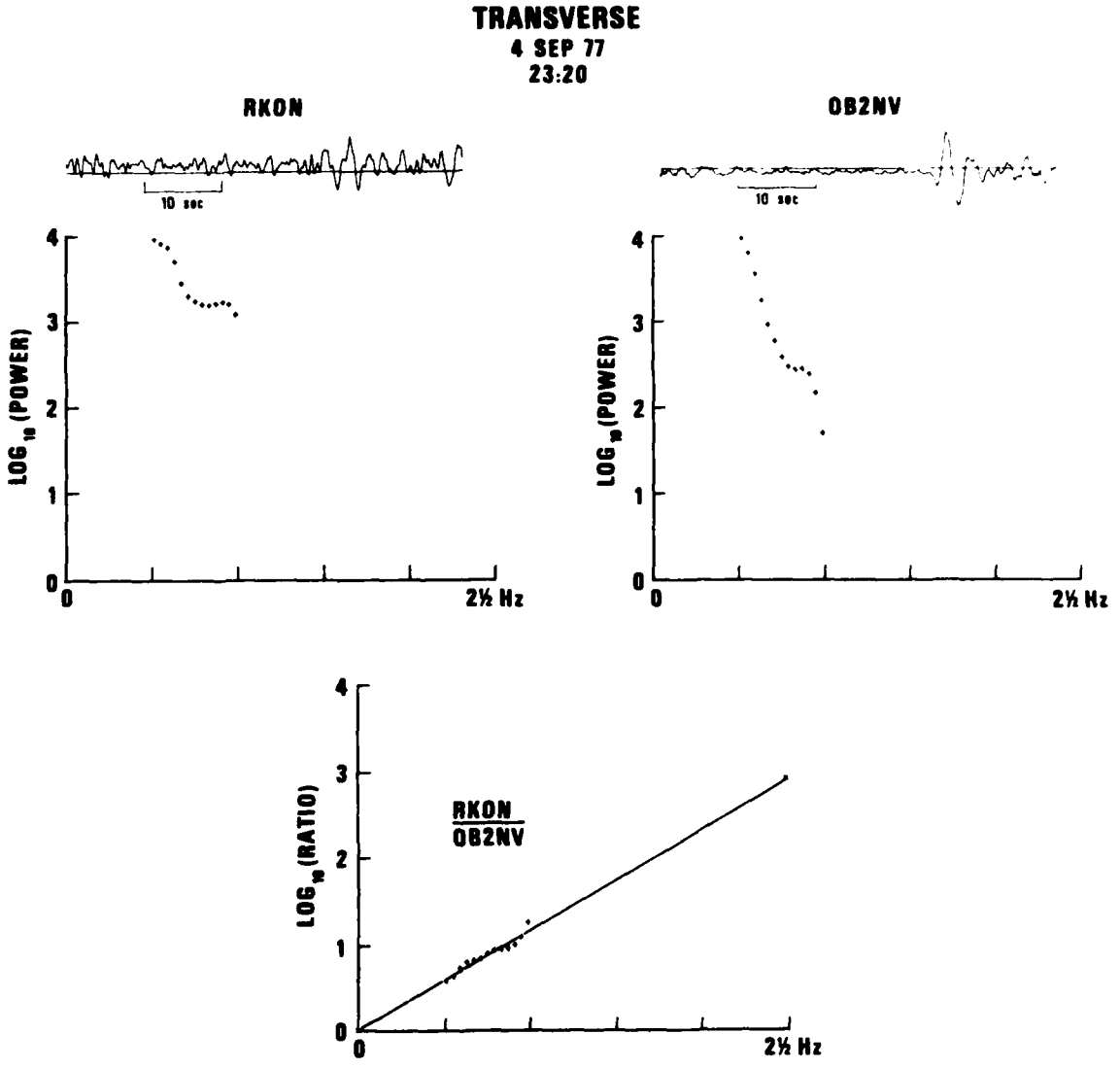

Figure 27. Time traces, power spectra and power spectral ratios for short period S waves observed at SDCS stations RKON and OB2NV, 4 September 1977 event, transverse component.

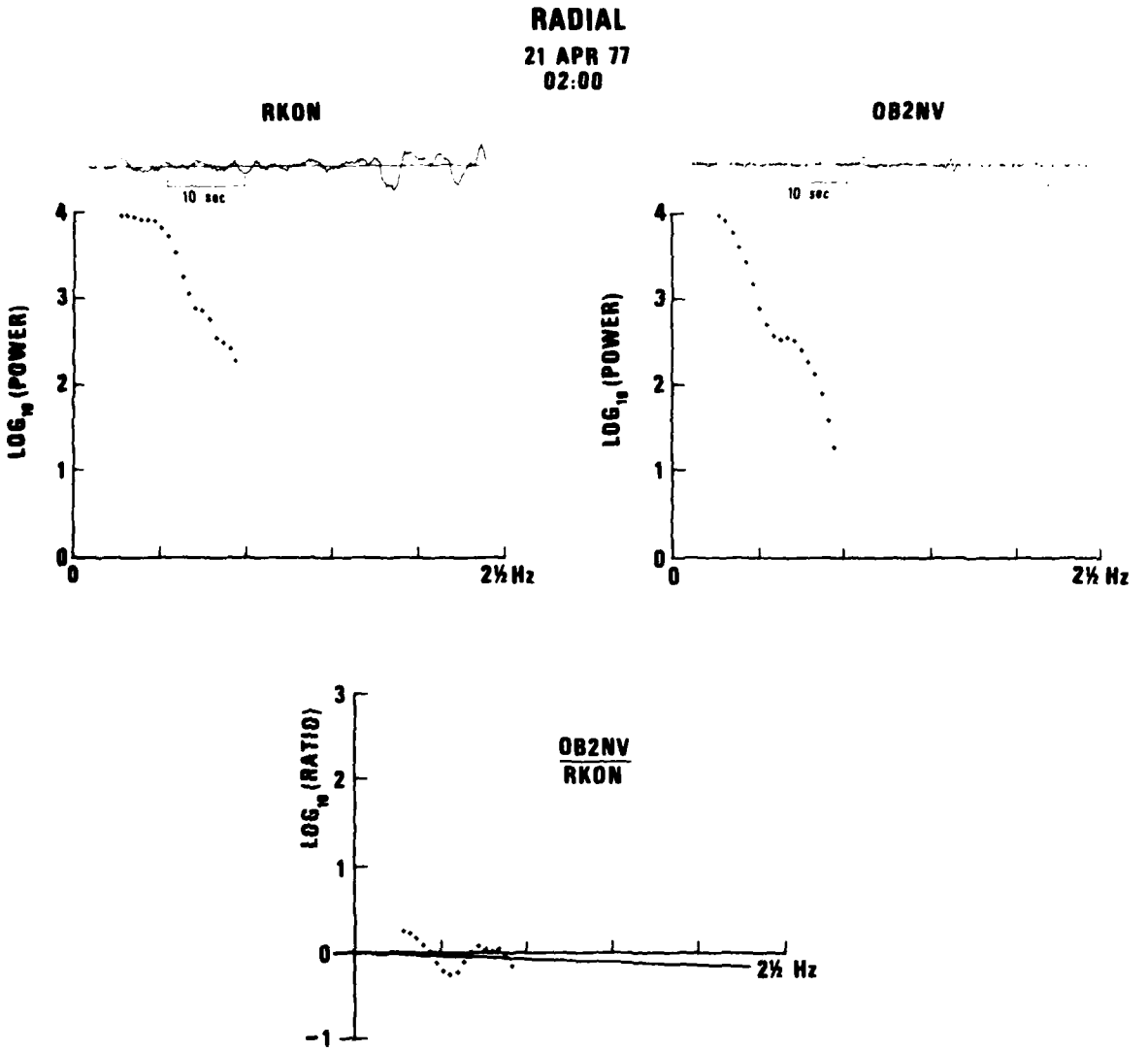

Figure 28. Time traces, power spectra and power spectral ratios for short period S waves observed at SDCS stations RKON and OB2NV, 21 April 1977 event, radial component.

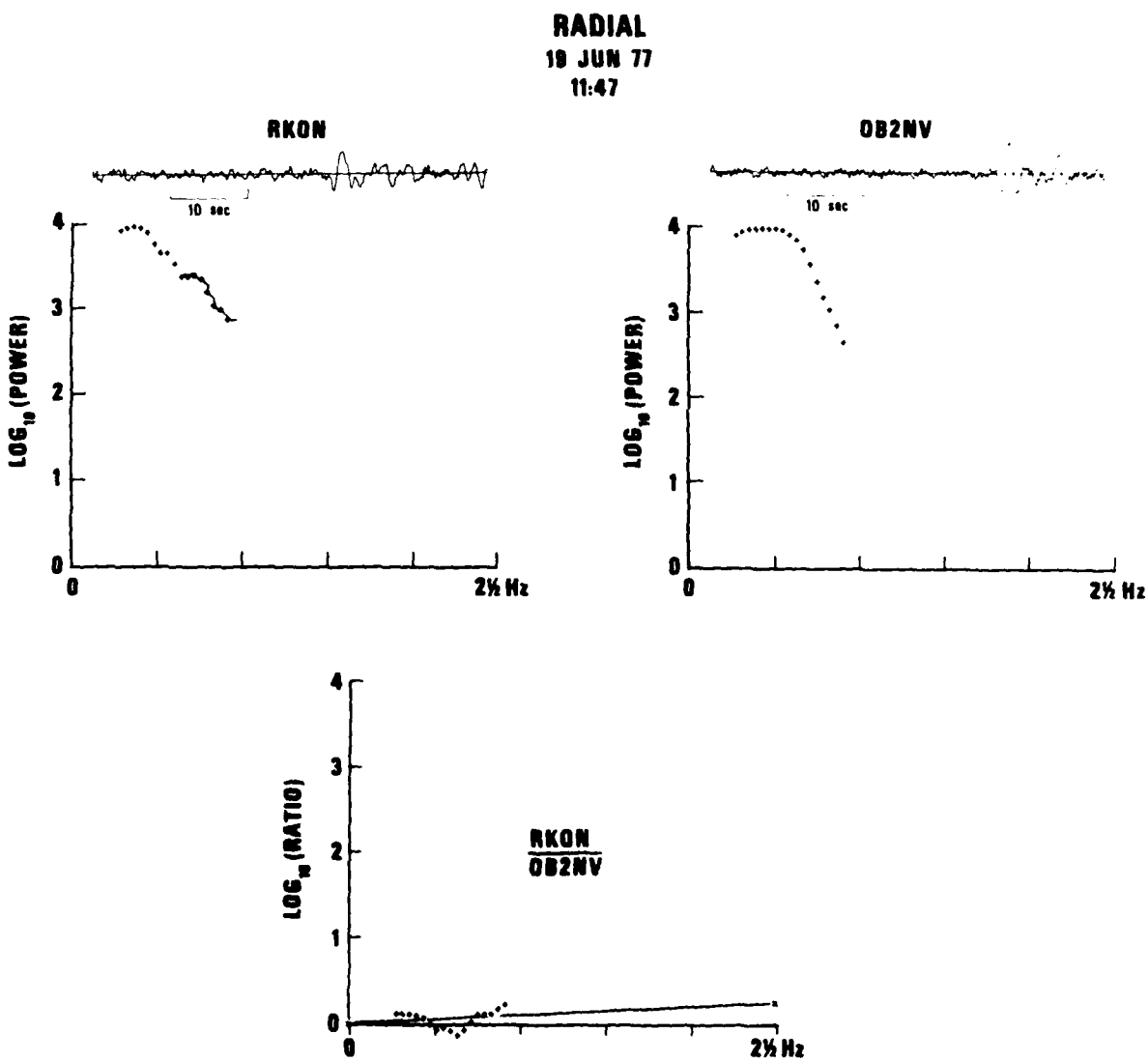

Figure 29. Time traces, power spectra and power spectral ratios for short period S waves observed at SDCS stations RKON and OB2NV, 19 June 1977 event, radial component.

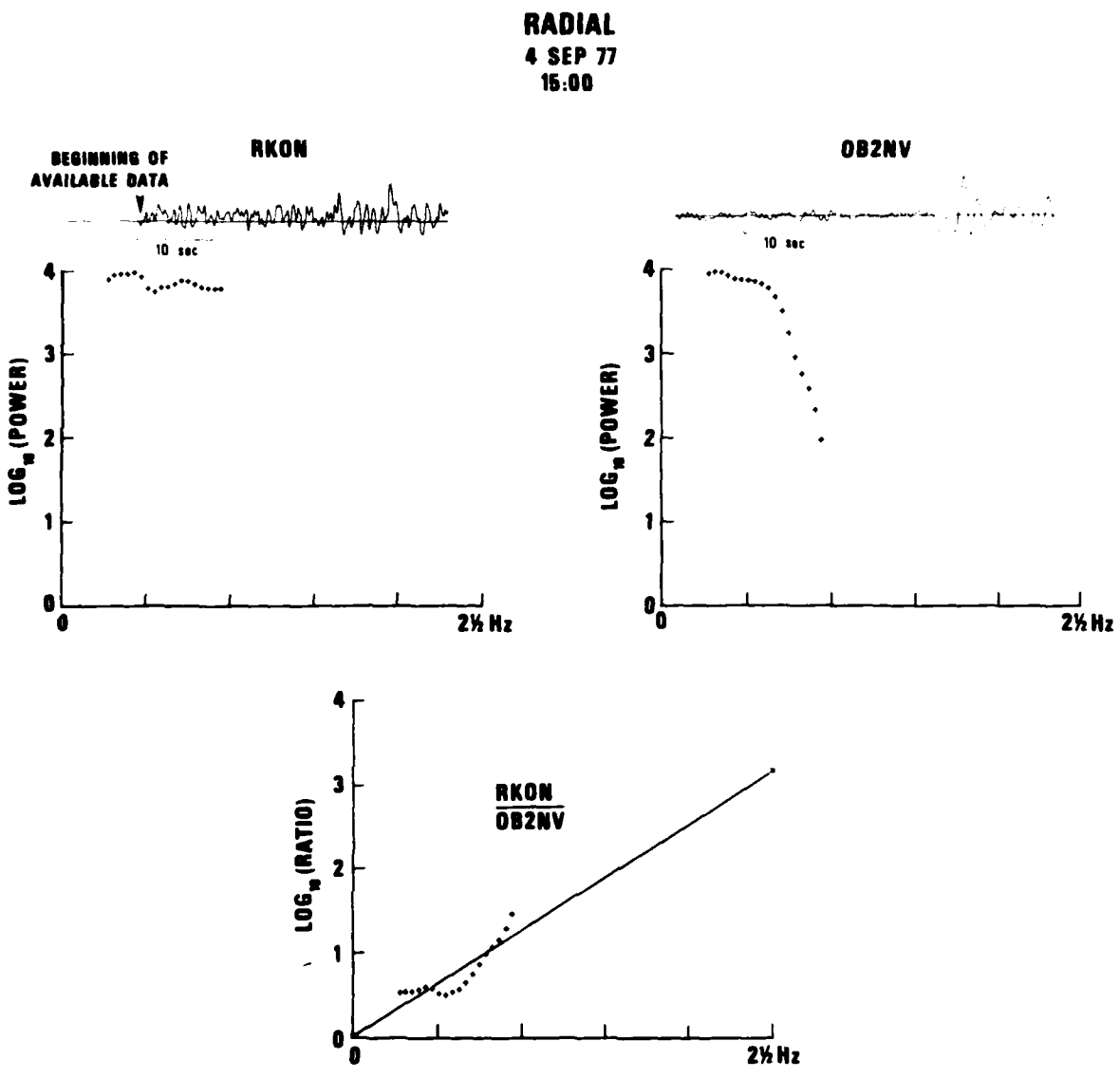

Figure 30. Time traces, power spectra and power spectral ratios for short period S waves observed at SDCS stations RKON and OB2NV, 4 September 1977 event, radial component.

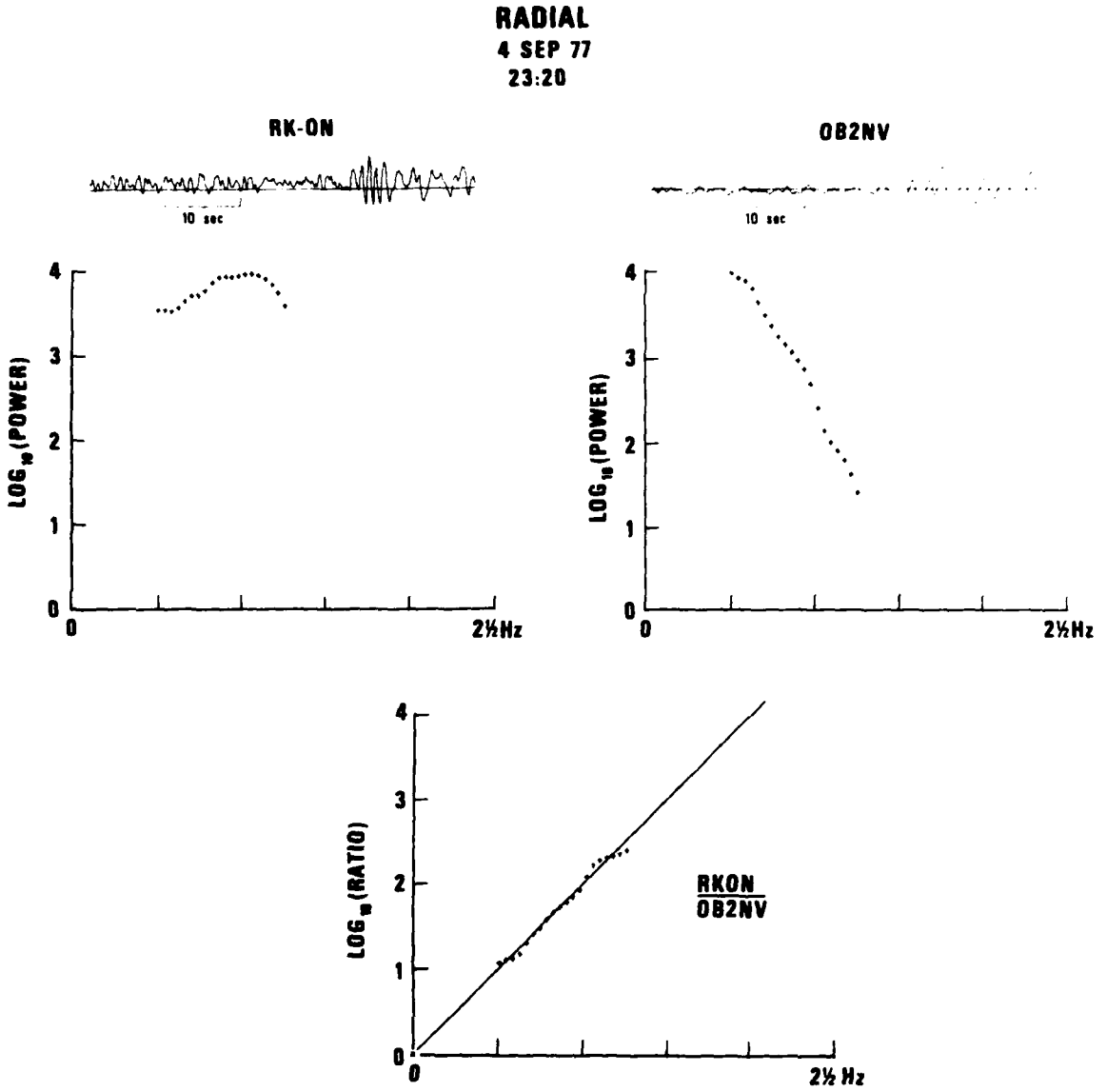

Figure 31. Time traces, power spectra and power spectral ratios for short period S waves observed at SDCS stations RKON and OB2NV, 4 September 1977 event, radial component.

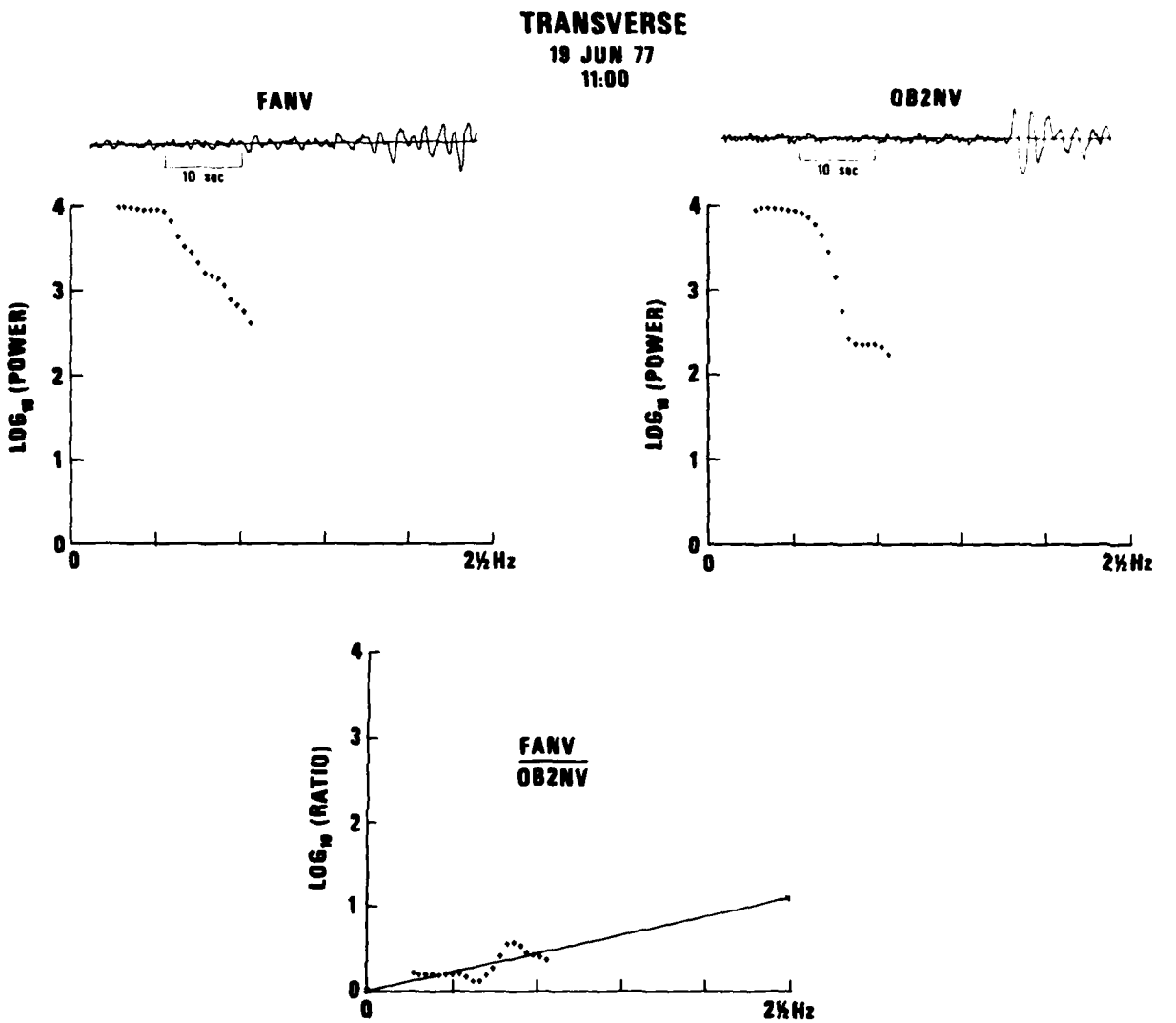

Figure 32. Time traces, power spectra and power spectral ratios for short period S waves observed at SDCS stations FANV and OB2NV, 19 June 1977 event, transverse component.

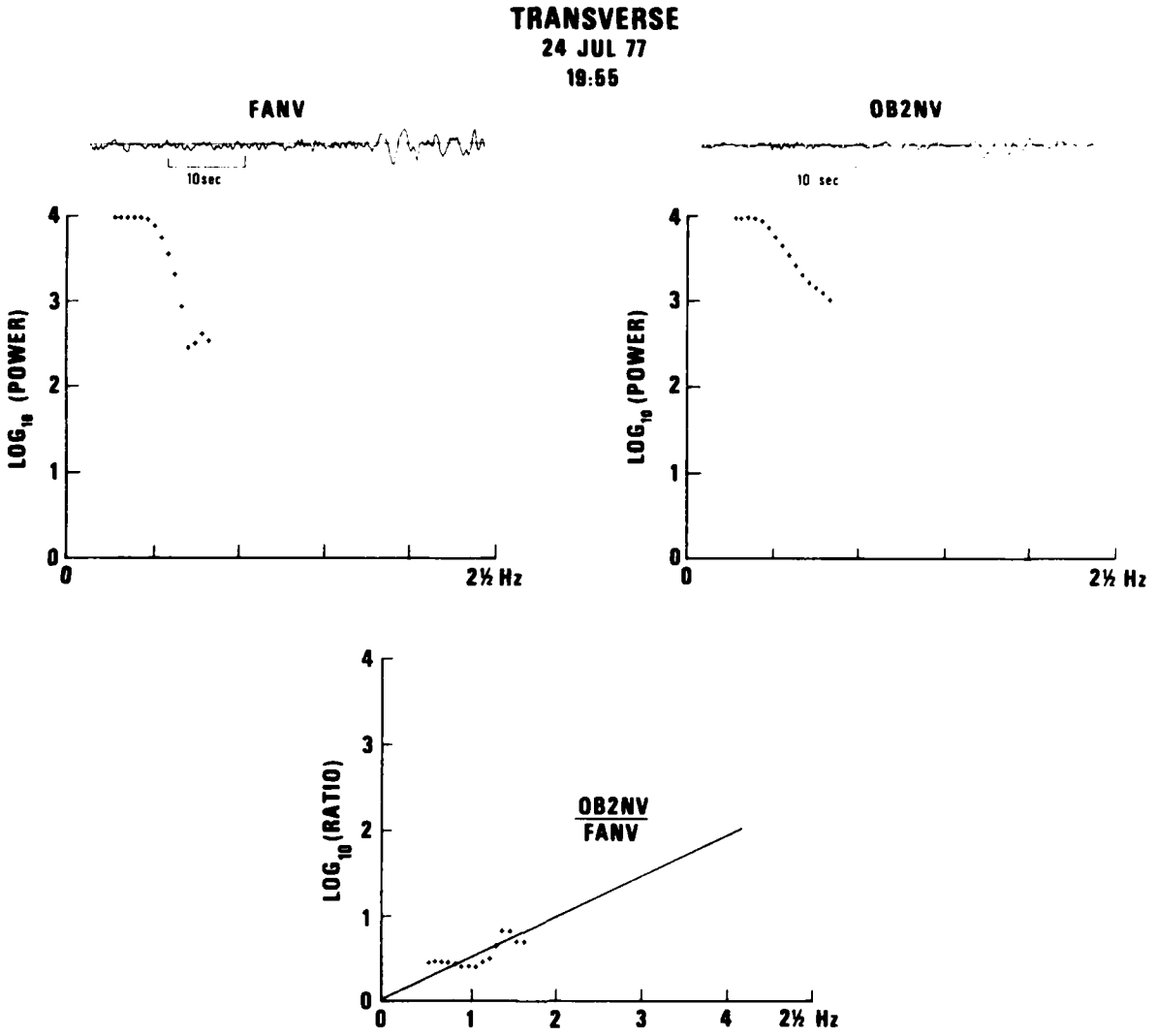

Figure 33. Time traces, power spectra and power spectral ratios for short period S waves observed at SDCS stations FANV and OB2NV, 21 July event, transverse component.

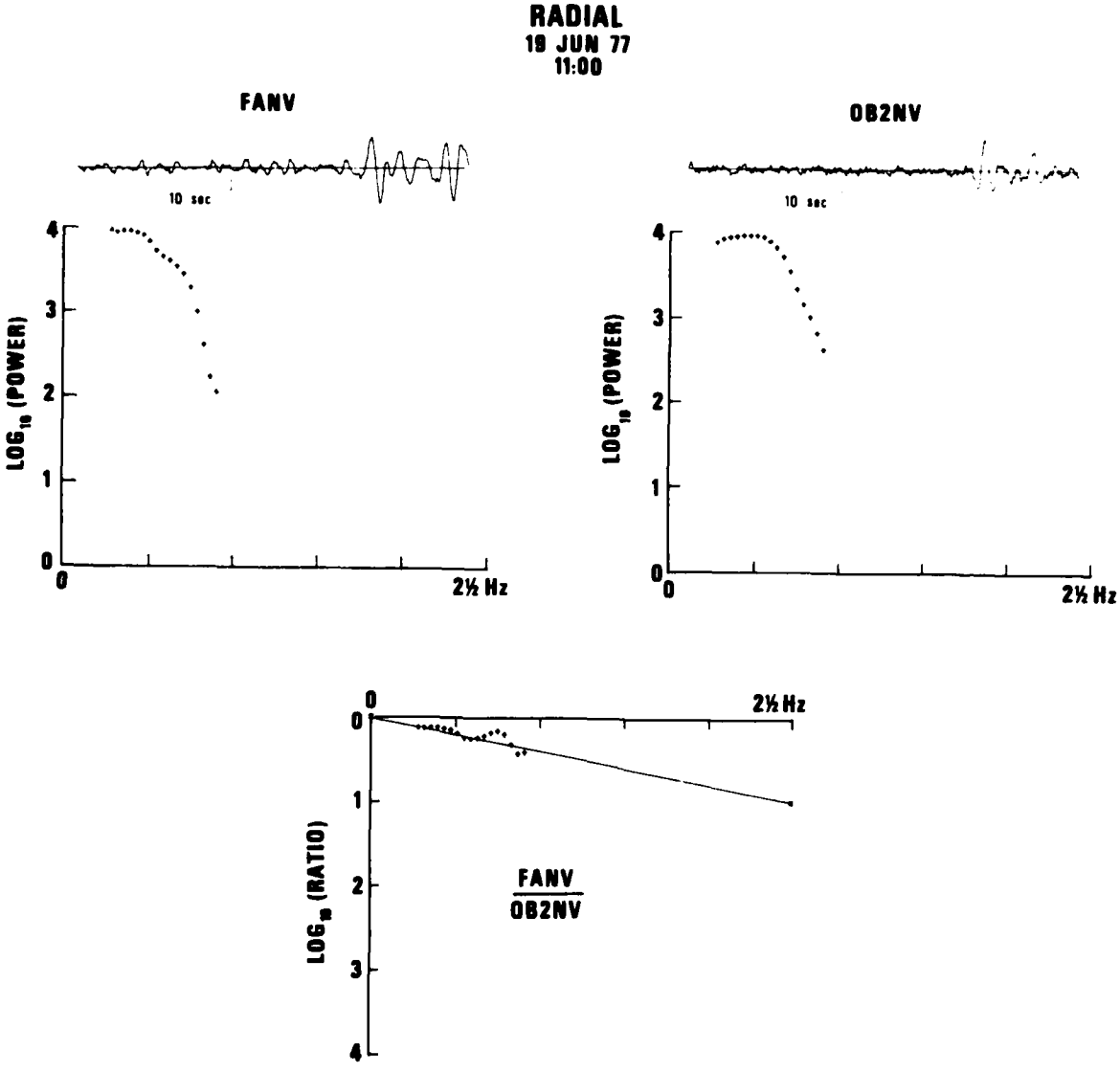

Figure 34. Time traces, power spectra and power spectral ratios for short period S waves observed at SDCS station FANV and OB2NV, 19 June 1977 event, radial component.

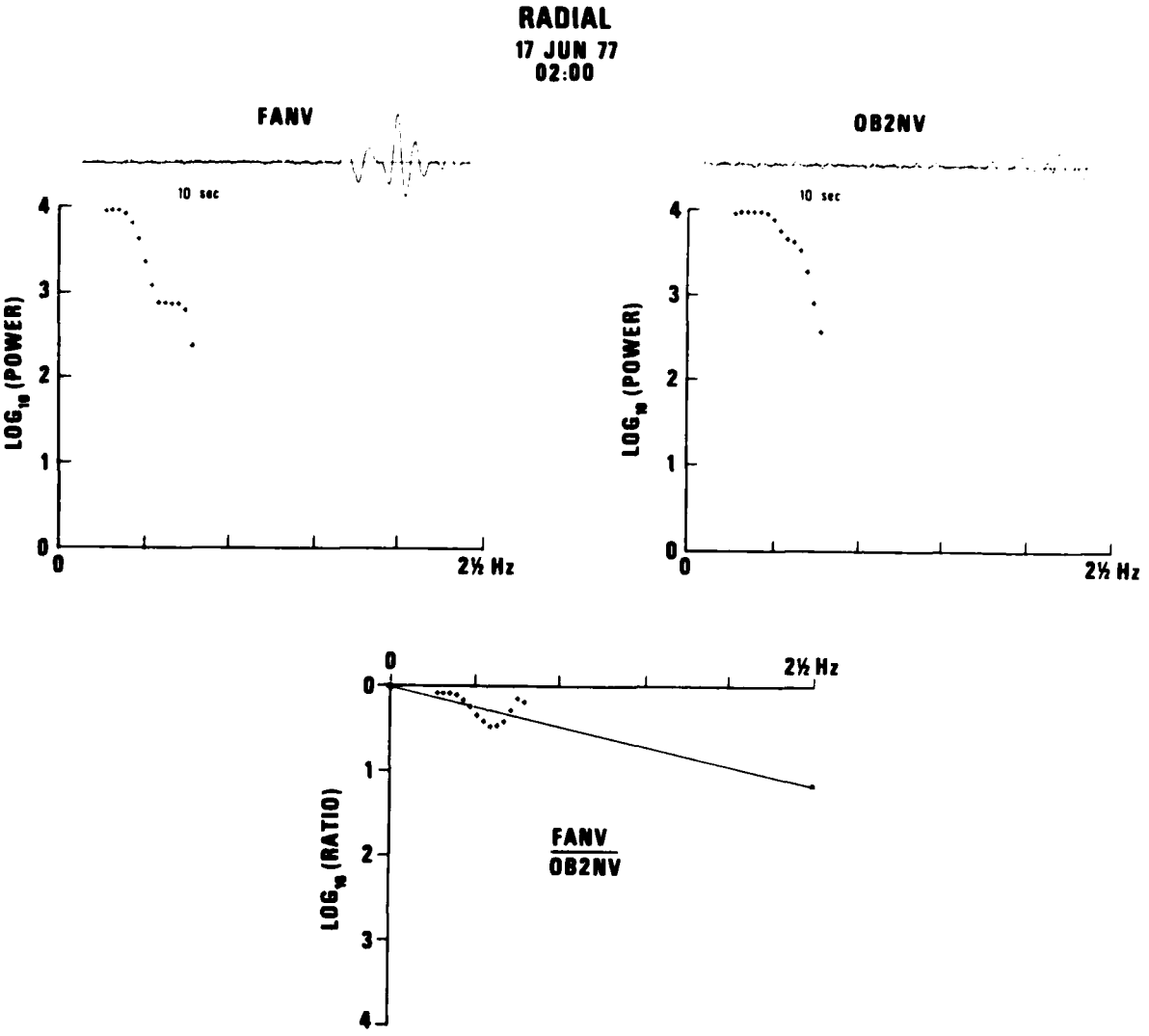

Figure 35. Time traces, power spectra and power spectral ratios for short period S waves observed at SDCS stations FANV and OB2NV, 17 June 1977 event, radial component.

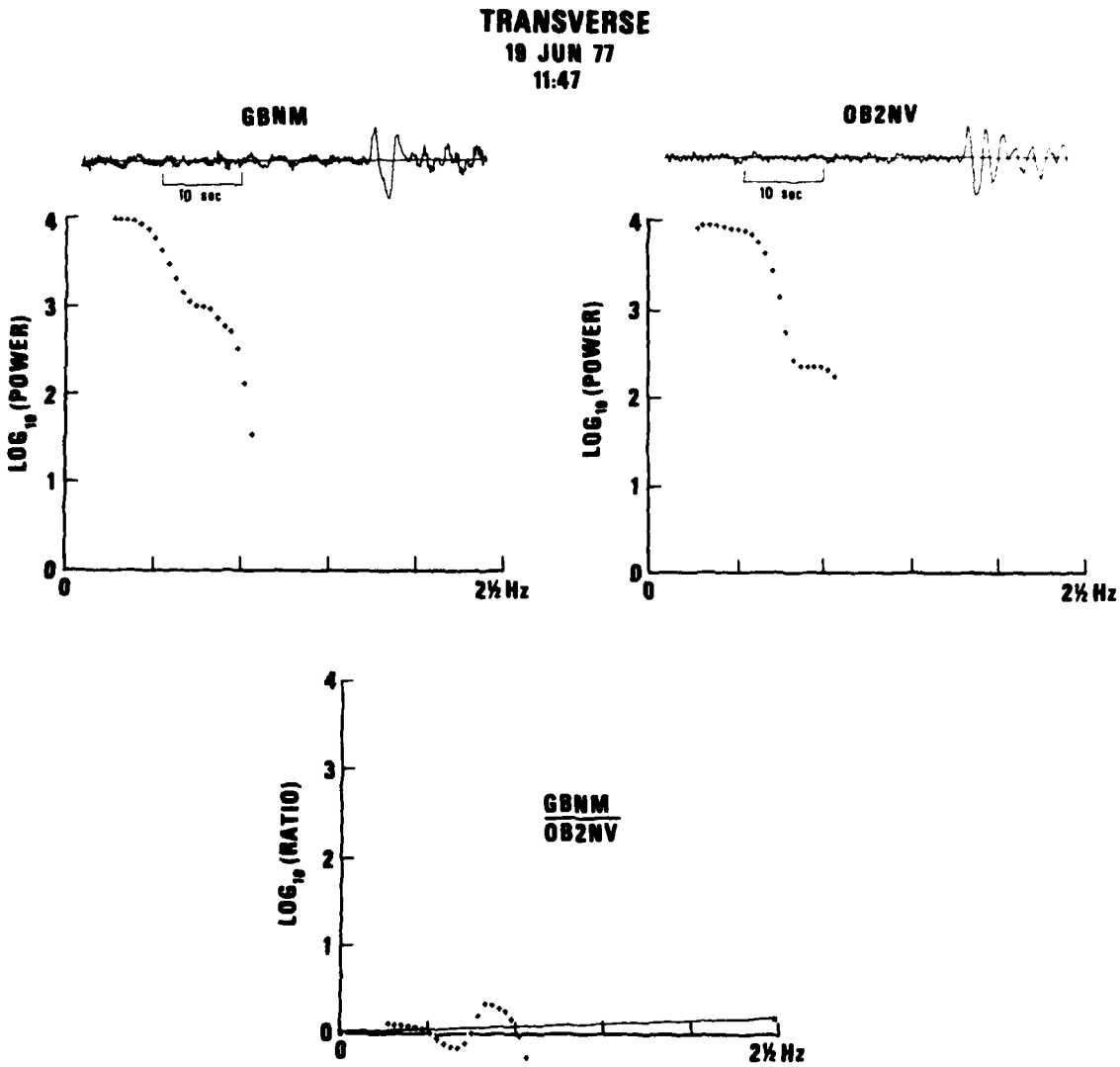

Figure 36. Time traces, power spectra and power spectral ratios for short period S waves observed at SDCS stations GBNM and OB2NV, 19 June 1977 event, transverse component.

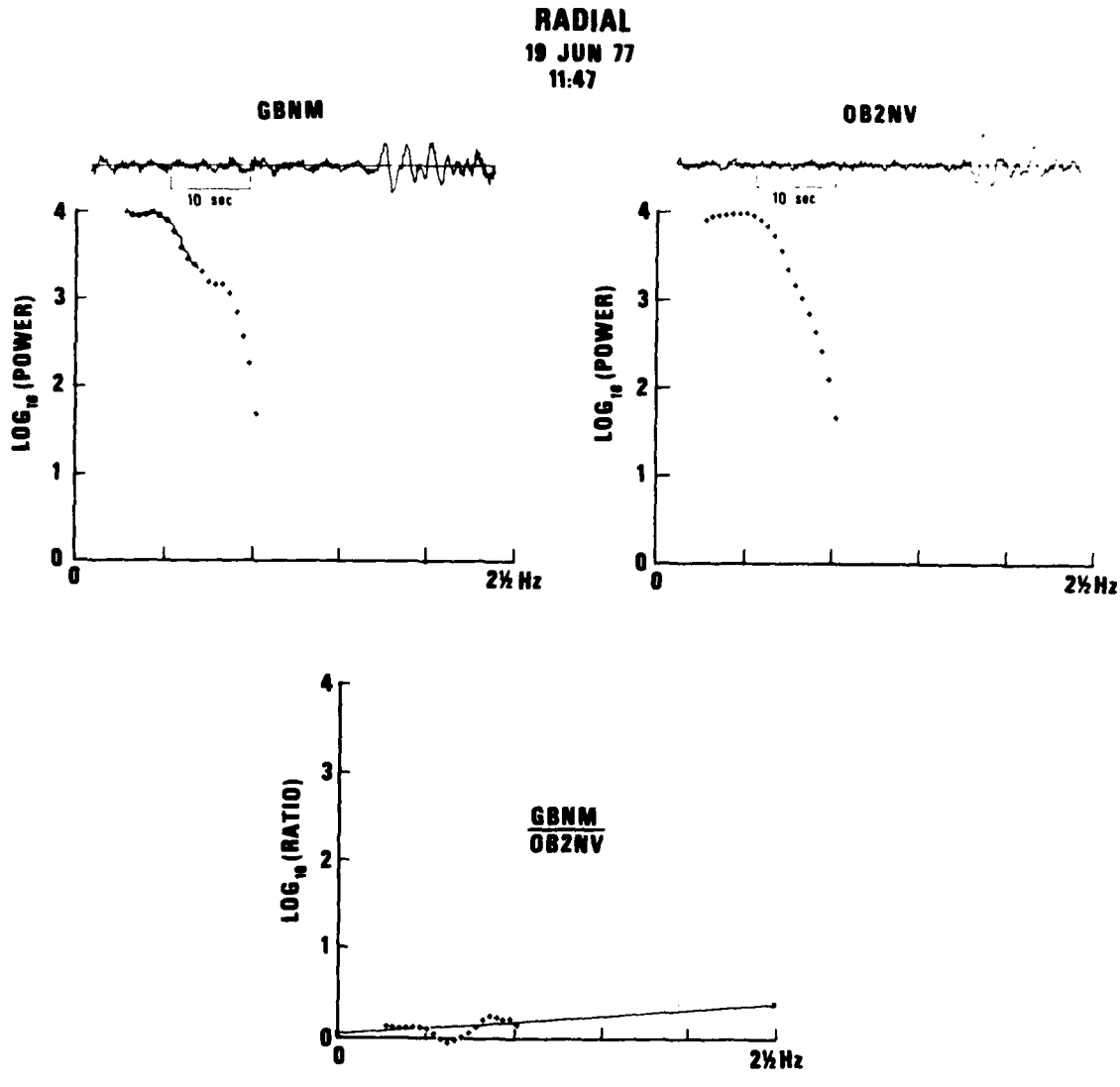

Figure 37. Time traces, power spectra and power spectral ratios for short period S waves observed at SDCS stations GBNM and OB2NV, 19 June 1977 event, radial component.

TABLE X

Relative Δt^* for short-period S-waves as seen at RKON and OB2NV.

	OB2NV/RKON	
	Transverse	Radial
April 21, ~ 0200 GMT	-0.198	0.238
June 19, ~ 1100 GMT	0.589	0.075
Sept. 4, ~ 1500 GMT	0.946	0.924
Sept. 4, ~ 2300 GMT	0.858	1.481
Mean	.549	.680

$\mu_T = 0.549$ $\mu_R = 0.680$

Mean $\Delta t_S^* = .615$

TABLE XI

Relative Δt^* for short-period S-waves as seen at FANV and OB2NV.

	FANV/OB2NV	
	Transverse	Radial
June 19, ~ 1100 GMT	-0.328	+0.293
July 24, ~ 1900 GMT	+0.484	
June 17, ~ 0200 GMT		+0.340

$$\Delta t^*_s = +.197$$

TABLE XII

Relative Δt^* for short-period S-waves as seen at GBNM and OB2NV.

	GBNM/OB2NV	
	Transverse	Radial
June 19, ~ 1100 GMT	-0.050	-0.107

$$\Delta t_s^* = -0.079$$

data. Spectral ratios for the FANV/OB2NV pair, four in all, indicate that FANV may have higher attenuation in the underlying mantle compared to OB2NV. However, the Δt^*_α difference would be only $\sim \Delta t^*_\beta/4 = 0.05$. The two spectral ratios for the GBNM/OB2NV pair show no appreciable spectral differences between the two stations. Though the data presented for NTS is meager, it demonstrates that NTS is similar to the rest of WUS. The average $\Delta t^*_s = .615$ for the OB2NV/RKON pair is similar to the regional EUS-WUS t^*_s difference obtained above. Although it is possible that the mantle under NTS, which is located close to the edge of the Colorado Plateau, could be less attenuating than the mantle under the rest of Basin and Range, the data above do not support this idea. The authors are continuing their search for more S wave data at the presently operating Seismic Data Collection System (SDCS) stations.

CONCLUSIONS

Results presented here provide additional evidence of high anelastic attenuation in the upper mantle under the WUS in general, and the SDCS station located in the WUS, in particular. In addition, the data also shed light on the attenuation mechanism, indicating that most of the losses occur in shear deformation, as expected for partially molten material (Walsh, 1968; Walsh, 1969). Losses in compressional deformation, if any, are likely to be small.

The actual attenuation mechanism is still being investigated theoretically. The basis for constructing theoretical models of attenuation is to assume some kind of mix of solids and viscous fluids in the upper mantle. The details of models vary; basic types are fluid inclusions in a solid (Walsh, 1968, 1969) and various mixes of solids and fluids with pores interconnected in various degrees and interfaces of various shapes (Anderson and Sammis, 1970; Budiansky and O'Connell, 1976; O'Connell and Budiansky, 1974, 1977; Spetzler and Anderson, 1968). The site of fluid-solid mix is thought to be the upper mantle low velocity zone, wherever it is present (Gueguen

---

Walsh, J. B. (1968). Attenuation in partially melted material, J. Geophys. Res., 73, 2209-2216.

Walsh, J. B. (1969). New analysis of attenuation in partially melted rock, J. Geophys. Res., 74, 4333-4337.

Anderson, D. L. and C. Sammis (1970). Partial melting in the upper mantle, Phys. Earth Planet. Interiors, 3, 41-50.

Budiansky, B., and R. J. O'Connell (1976). Elastic moduli of dry and saturated cracked solids, Int. J. Solids Struct., 12, 81-97.

O'Connell, R. J. and B. Budiansky (1974). Seismic velocities in dry and saturated cracked solids. J. Geophys. Res., 79, 5412-5426.

O'Connell, R. J. and B. Budiansky (1977). Measures of attenuation in dissipated media, submitted to Geophys. Res. Lett.

Spetzler, H. A. and D. L. Anderson (1968). The effect of temperature and partial melting on velocity and attenuation in a simple binary system, J. Geophys. Res., 73, 6051-6060.

and Mercier, 1973; Anderson and Spetzler, 1970; Solomon, 1972). All models essentially behave as superpositions of standard linear solids, with many non-overlapping frequency bands to account for the near constancy of Q with frequency, but allowing some increase of Q at frequencies above 1 Hz to make it agree with a higher Q observed there (O'Connell and Budiansky, 1974, 1977; Solomon, 1972; Anderson and Hart, 1976). The data presented here cannot be used to decide which proposed attenuation mechanism is actually operating in the upper mantle. The common assumption, the presence of a solid-viscous fluid mix in the upper mantle, is supported by a broad range of geophysical data recently reviewed by Der (1976) and others (Herrin, 1972, for example).

Gueguen, Y., and J. M. Mercier (1973). High attenuation and the low-velocity zone, Phys. Earth Planet. Interiors, 7, 39-46.

Anderson, D. L. and H. Spetzler (1970). Partial melting in the low-velocity zone, Phys. Earth Planet. Interiors, 4, 62-64.

Anderson, D. L., and R. S. Hart (1976). An earth model based on free oscillations and body waves, J. Geophys. Res., 81, 1461-1475.

Herrin, E. (1972). A comparative study of upper mantle models, Canadian Shield and Basin and Range provinces, in The Nature of the Solid Earth, E. C. Robertson, Editor, New York, McGraw-Hill.

Der, A. Z. (1976). On the existence, magnitude and causes of broad regional variations in body-wave amplitudes (magnitude bias), SDAC-TR-76-8, Teledyne Geotech, Alexandria, Virginia 22314.

ACKNOWLEDGEMENTS

The authors gratefully acknowledge help from the Data Services Group under John Woolson in organizing and digitizing the data. Tom McElfresh assisted in programming. Drs. Shelton Alexander and Robert Blandford reviewed the paper and made helpful suggestions.

REFERENCES

Anderson, D. L., and R. S. Hart (1976). An earth model based on free oscillations and body waves, J. Geophys. Res., 81, 1461-1475.

Anderson, D. L., and C. Sammis (1970). Partial melting in the upper mantle, Phys. Earth Planet. Interiors, 3, 41-50.

Anderson, D. L., and H. Spetzler (1970). Partial melting in the low-velocity zone, Phys. Earth Planet. Interiors, 4, 62-64.

Budiansky, B., and R. J. O'Connell (1976). Elastic moduli of dry and saturated cracked solids, Int. J. Solids Struct., 12, 81-97.

Berckhemer, H., and K. H. Jacob (1968). Investigation of the dynamical process in earthquake foci by analyzing the pulse shape of body waves, Final Scientific Report, Institute of Meteorology and Geophysics, University of Frankfurt, Germany, AD738953

Der, Z. A. (1976). On the existence, magnitude and causes of broad regional variations in body-wave amplitudes (magnitude bias), SDAC-TR-76-8, Teledyne Geotech, Alexandria, Virginia 22314.

Der, Z. A., R. P. Massé, and J. P. Gurski (1975). Regional attenuation of short-period P and S waves in the United States, Geophys. J., 40, 85-106.

Der, Z. A., and T. W. McElfresh (1977). The relationship between anelastic attenuation and regional amplitude anomalies of short-period P waves in North America, Bull. Seism. Soc. Am., 67, 1303-1317.

Evernden, J., and D. M. Clark (1970). Study of teleseismic P. II amplitude data, Phys. Earth Planet. Interiors, 4, 24-31.

Gueguen, Y., and J. M. Mercier (1973). High attenuation and the low-velocity zone, Phys. Earth Planet. Interiors, 7, 39-46.

Guyton, J. W. (1964). Systematic deviations of magnitude from body waves at seismograph stations in the United States, Proc. VESIAC Conf. Seismic Event Magnitude Determination, University of Michigan, 4410-71-X.

Herrin, E. (1972). A comparative study of upper mantle models, Canadian Shield and Basin and Range provinces, in The Nature of the Solid Earth, E. C. Robertson, Editor, New York, McGraw-Hill.

Mendiguren, J. A. (1969). Study of focal mechanism of deep earthquakes in Argentina using nonlinear particle motion of S waves, Bull. Seism. Soc. Am., 59, 1449-1473.

North, R. G. (1977). Station magnitude biases-its determination, causes and effects, Lincoln Laboratory, M.I.T. Technical Note 1977-24, 62.

O'Connell, R. J., and B. Budiansky (1974). Seismic velocities in dry and saturated cracked solids, Int. J. Solids Struct., 12, 81-97.

O'Connell, R. J., and B. Budiansky (1977). Measures of attenuation in dissipative media, submitted to Geophys. Res. Lett.

Sengupta, M. K. and M. N. Toksöz (1977). The amplitudes of P waves and magnitude corrections for deep focus earthquakes, J. Geophys. Res., 82, 2071-20 .

Solomon, S. C. (1972). Seismic-wave attenuation and partial melting in the upper mantle of North America, J. Geophys. Res, 77, 1483-1502.

Solomon, S. C., and M. N. Toksöz (1970). Lateral variations of attentuation of P and S waves beneath the United States, Bull. Seism. Soc. Am., 60, 819-838.

Spetzler, H. A., and D. L. Anderson (1968). The effect of temperature and partial melting on velocity and attenuation in a simple binary system, J. Geophys. Res., 73, 6051-6060.

Veith, K. F. (1974). The relationship of island arc seismicity to plate tectonics, Ph.D. thesis, Southern Methodist University, Dallas, Texas.

Walsh, J. B. (1968). Attenuation in partially melted material, J. Geophys. Res., 73, 2209-2216.

Walsh, J. B. (1969). New analysis of attenuation in partially melted rock, J. Geophys. Res., 74, 4333-4337.